

## PLATES

## PLATE I

a. Isoclinal folds in mica schists near San Finx. Narrow quartz-rich bands and folds ( $F_1$ ) underwent a second deformation by  $F_2$  as well as nearby fault movements. The older structures ( $F_1$ ) have been obliterated in the mica-rich parts of the sample (St. 141682).

b. A banded albiteblast-bearing paragneiss ( $s_1$ ) showing traces of a second deformation ( $s_2$ ). Negative print: the micas are white and the albites dark (St. 141692).

c. Thin section of a weakly banded paragneiss ( $F_1$ ) in which a weak second schistosity ( $s_2$ ) is visible. A tourmaline vein sub-parallel to  $s_1$  has also been folded by  $F_2$ . Negative print: tourmaline vein and micas are white, quartz and plagioclase are dark (St. 141691).

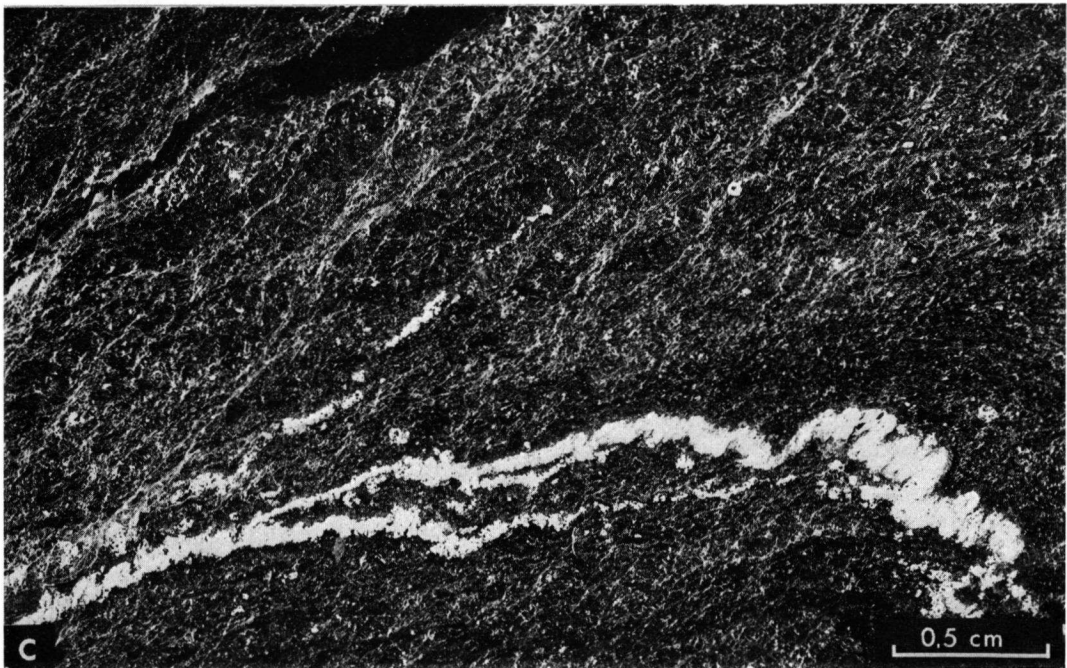
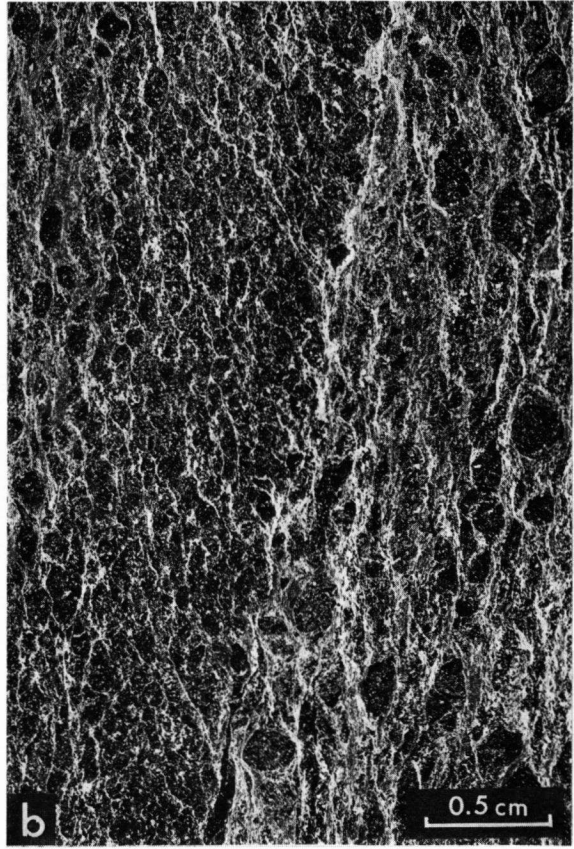


**PLATE II**

- a. Twinned oligoclase metablast, enclosing small quartz droplets, resorbed garnet and opaque minerals in metablastic paragneiss 1 km WSW of Pte. Beluso.
- b. An untwinned oligoclase metablast enclosing relatively large as well as some smaller quartz grains and a few micas; location 700 m ENE of Noya.
- c. A twinned albite metablast with quartz grains ( $s_1$ ) in parallel alignment in an albiteblast-bearing paragneiss 600 m WSW of Val.

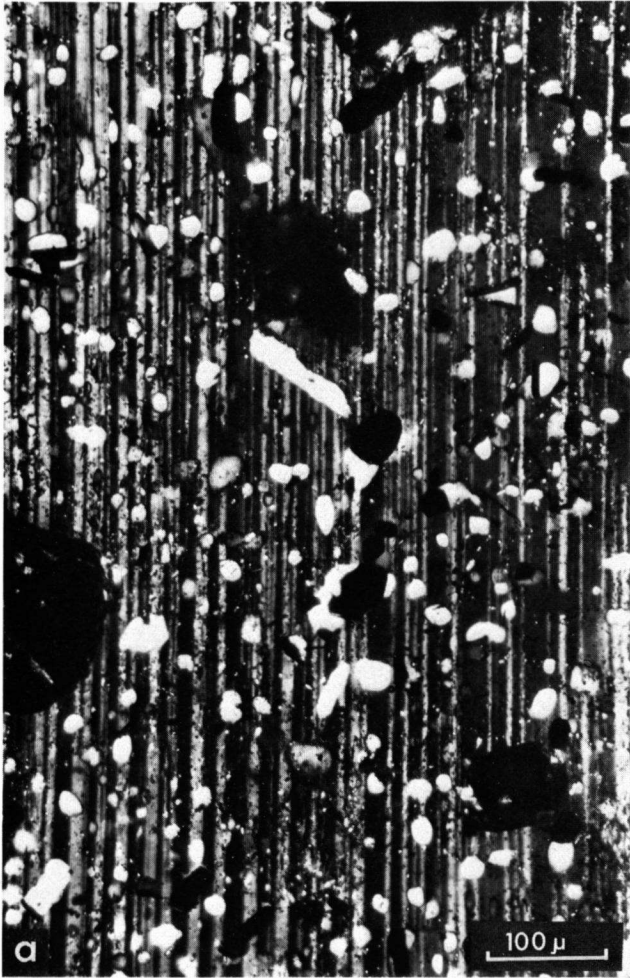
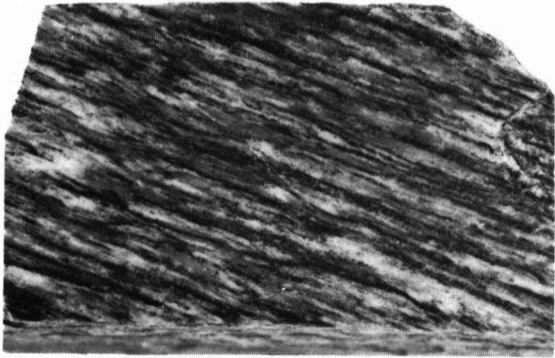


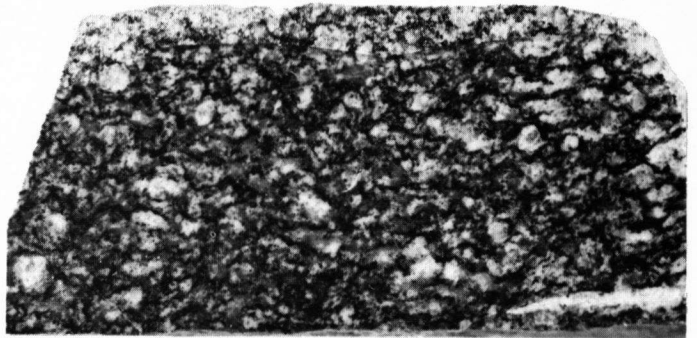
**PLATE III**

- a. Linear blastomylonitic biotite orthogneiss; section // lineation (St. 141717).
- b. Same sample, section  $\perp$  lineation.
- c. Planoliner biotite orthogneiss; section  $\perp$  foliation (St. 141720).
- d. Augen-bearing biotite orthogneiss. Part of the alkali feldspar augen have been completely crushed (Pta. Péon).
- e. Partly mobilized biotite orthogneiss (St. 141790).



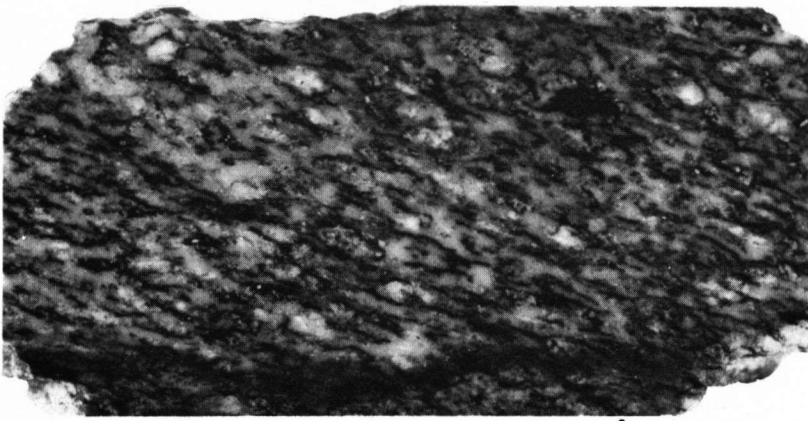
a

1cm



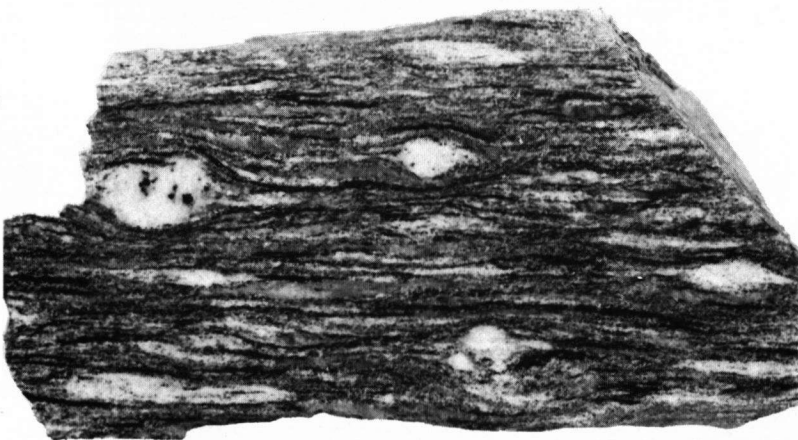
b

1cm



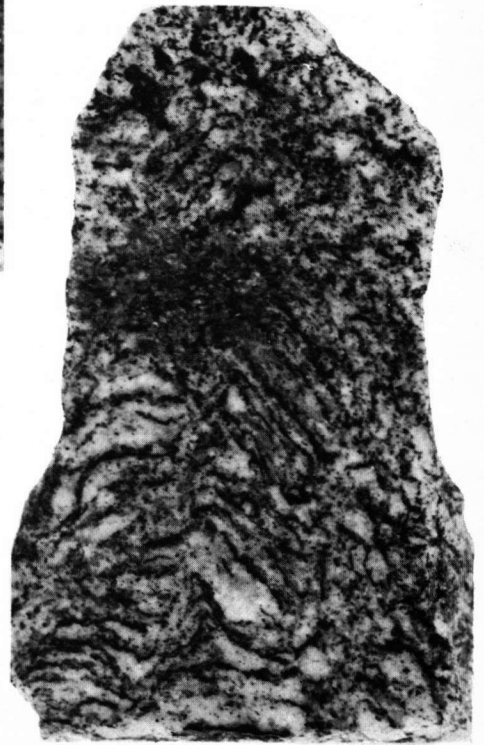
c

1cm



d

1cm



e

1cm

#### PLATE IV

a. Linear blastomylonitic biotite orthogneiss; photomicrograph (crossed nicols) of thin section // lineation. Quartz is highly recrystallized (post- $F_3$ ; mosaic or polygonal); the micas occur mainly in the microcrystalline mortar zones (white streaks). Negative print (St. 141717).

b. Thin section photomicrograph of the same sample  $\perp$  lineation. The recrystallized quartz aggregates are more coarsely grained than the feldspar aggregates. Negative print.

c. Thin section photomicrograph of an ortho-amphibolite displaying a metaporphyritic structure. The isometric relics are plagioclase aggregates which may often enclose biotites (St. 141745).

d. Photomicrograph of an ortho-amphibolite (St. 141745) with a metaporphyritic structure (hornblende clusters).



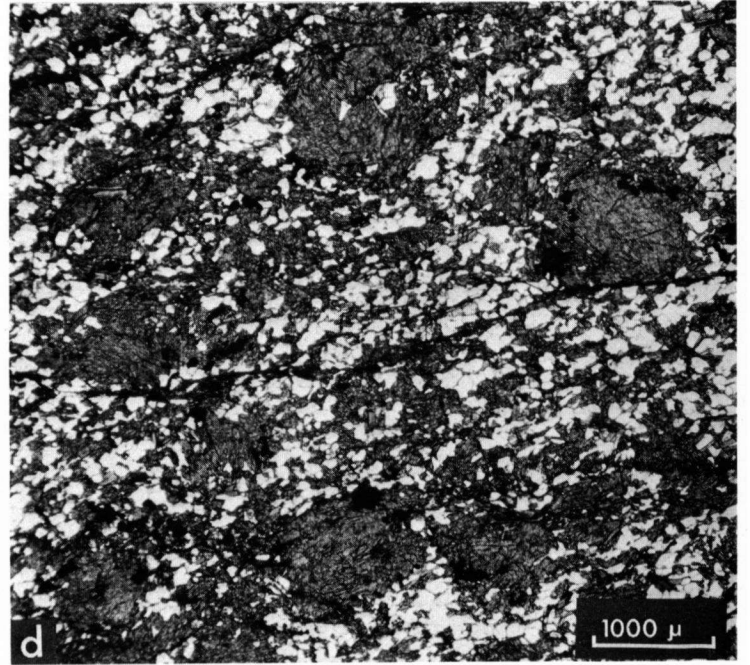
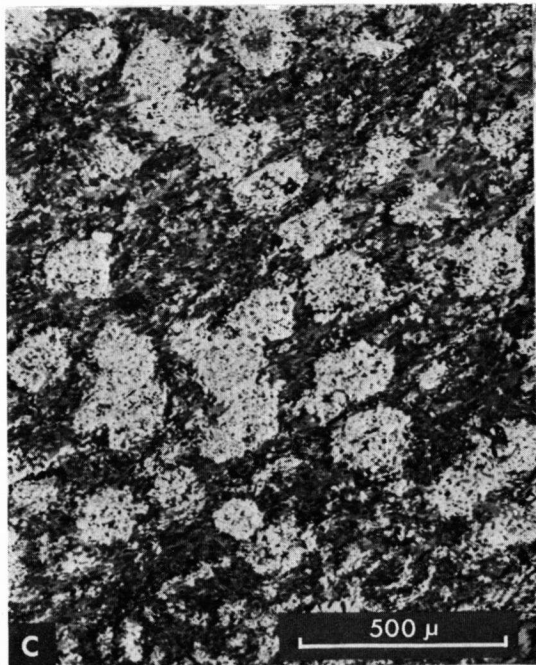
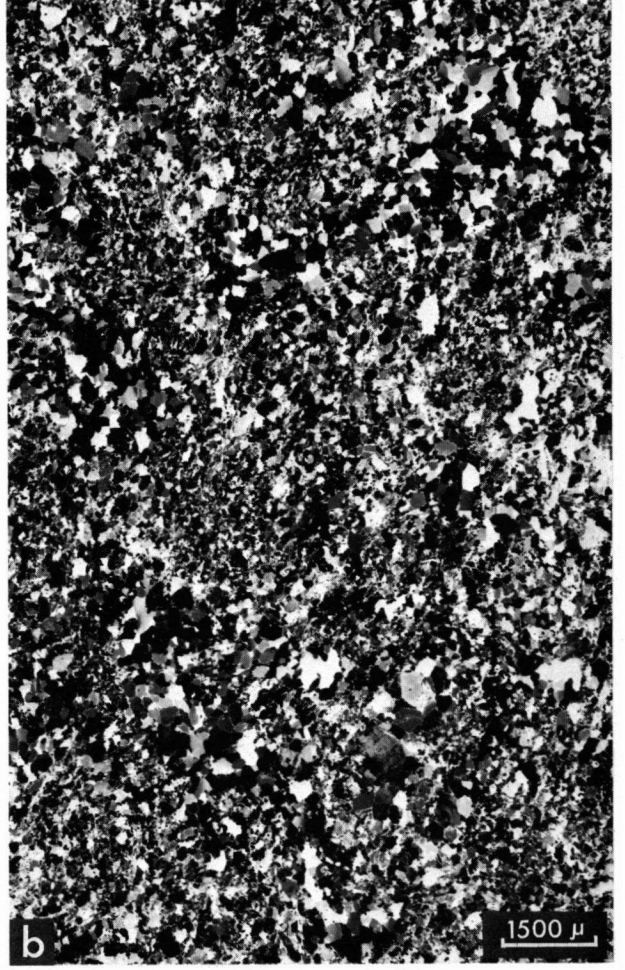
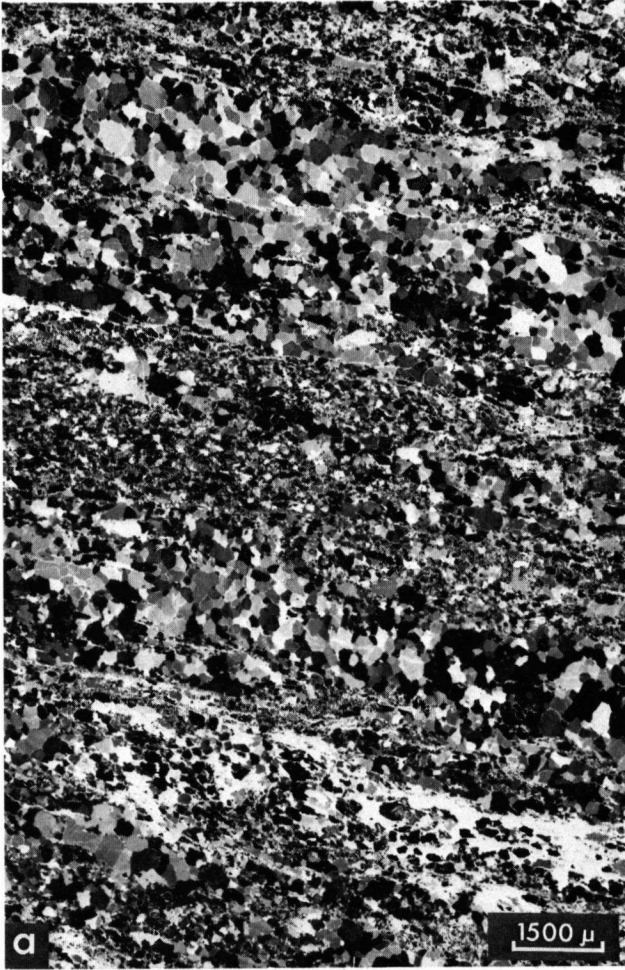


#### PLATE V

- a. A finely banded ( $s_1$ ) muscovite-chlorite-bearing metaquartzite deformed by  $F_2$ , resulting in a sub-vertical crenulation cleavage. A few large post-kinematic (with respect to  $F_2$ ) andalusite crystals have grown in the crenulation cleavage planes. Negative print: micas and andalusite are greyish or white; quartz is dark (St. 141703).
- b. An isoclinal  $F_1$ -fold in a graphite schist enclosing traces of pre- $F_1$  ( $F_0$ ?) folds in the crests. Negative print: graphite is white and quartz is dark (St. 141707).
- c. Albite metablast (aggregate) with a folded  $s_1$  (St. 141712).

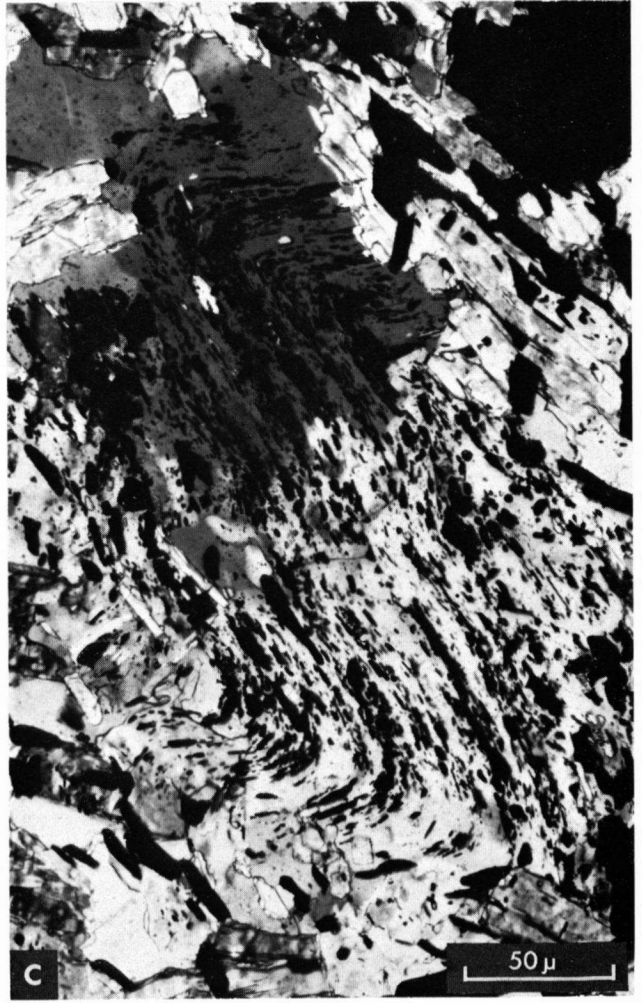
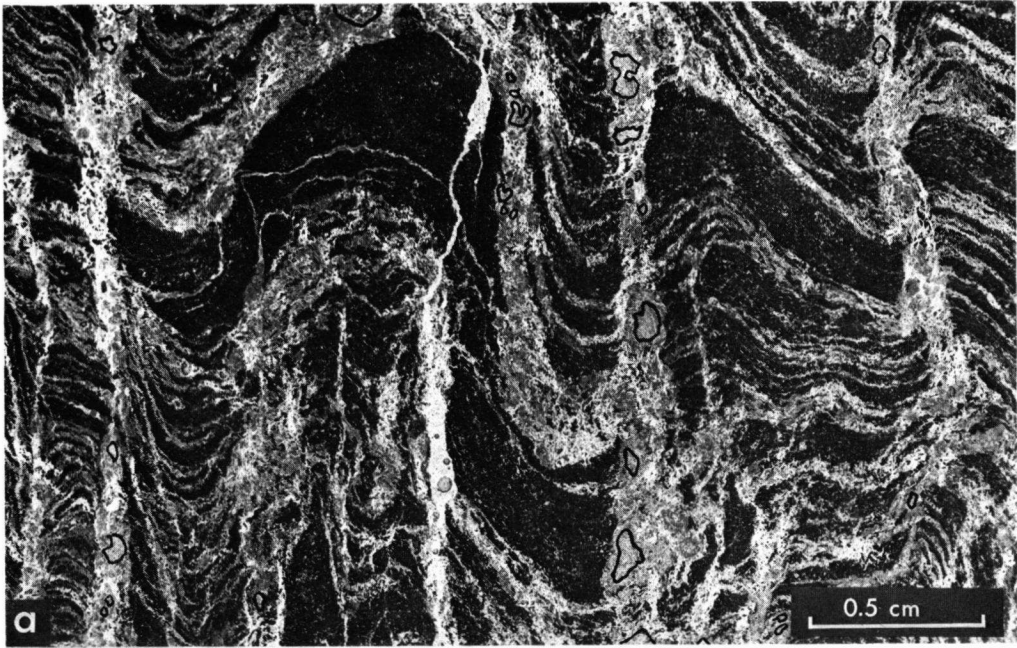
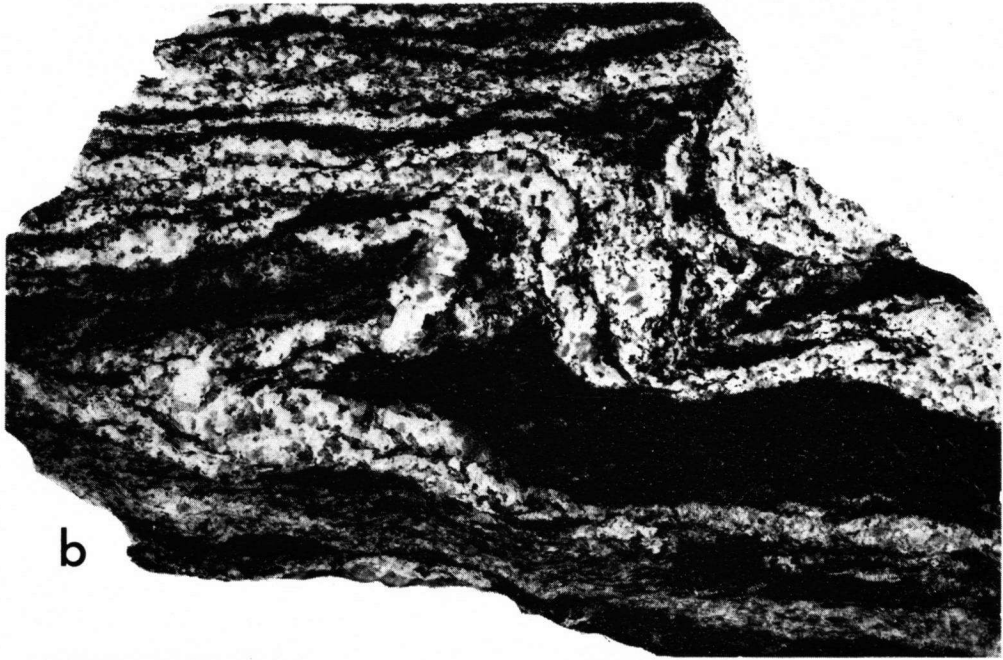
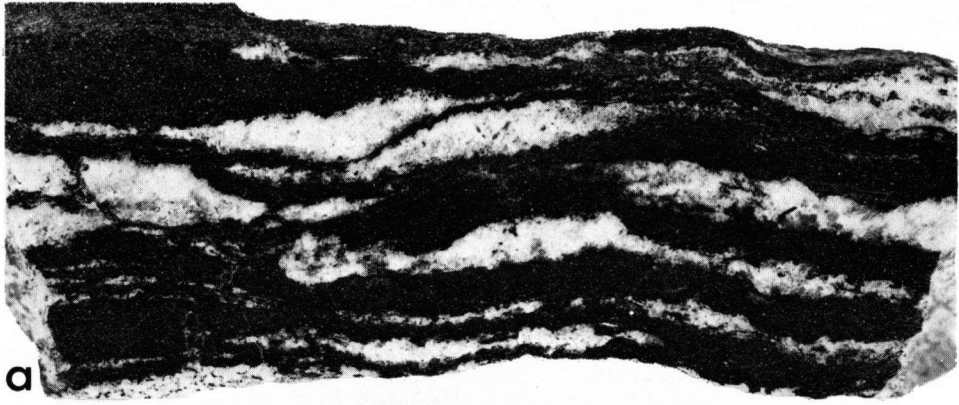


#### PLATE VI

- a. Migmatite with a banded structure (metatexite); the metatect consists of quartz and some plagioclase. Biotite has recrystallized in the melanosome where it borders the metatect (St. 141766).
- b. Migmatite with a folded structure. The metatect has a pegmatitic or granitic composition (St. 141775).
- c. Migmatite with a "schlieren" structure. The incoherent melanosome was folded because of the high mechanical mobility of the granitic metatect (location 4.8 km NE of Pte. Beluso).



1cm

**PLATE VII**

- a. Alkali feldspars displaying albitization and different types of perthite; granitoid migmatite, 5 km E of Val.
- b. Rim of a large alkali feldspar from a coarse-grained augengneiss, 7 km NNW of Esteiro, showing two successive stages during myrmekitization: the fine quartz wormlets close to the alkali feldspar and the recrystallized quartz drops farther away.

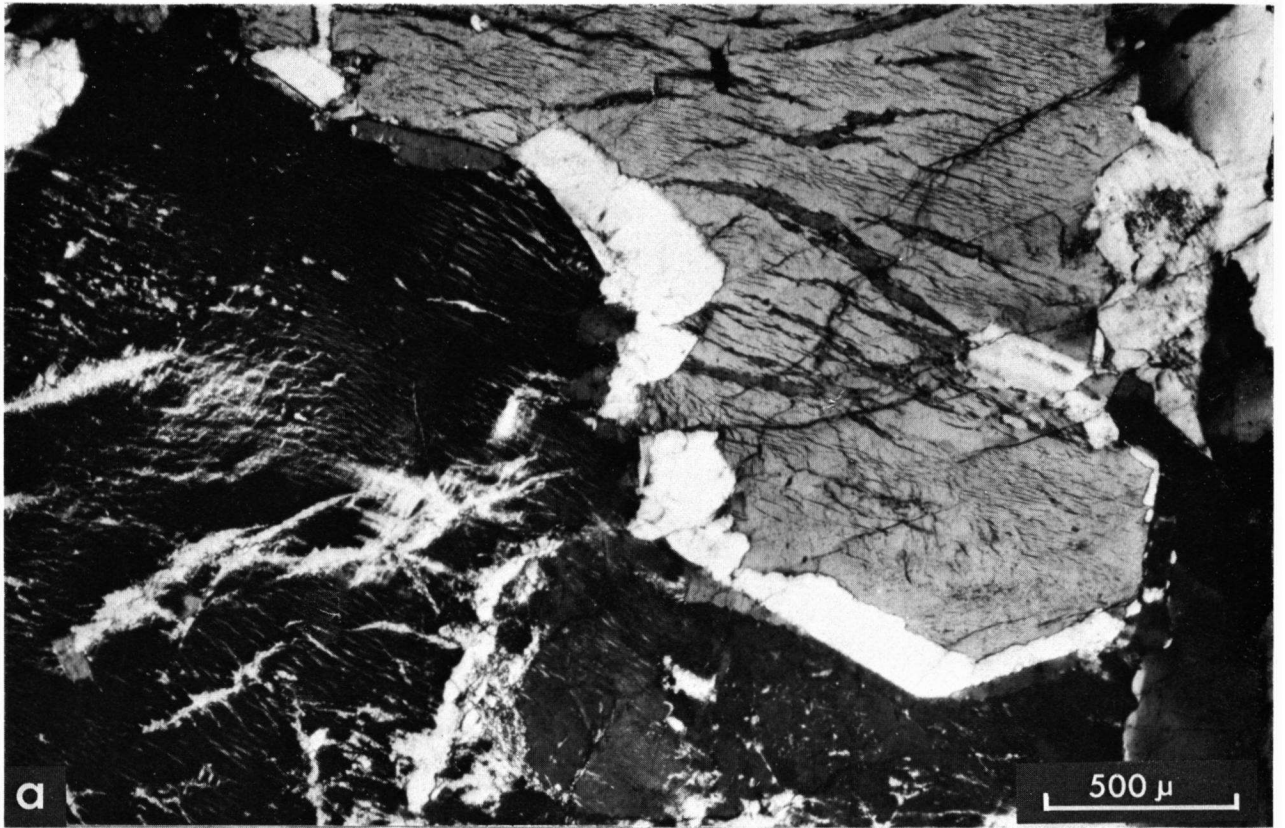
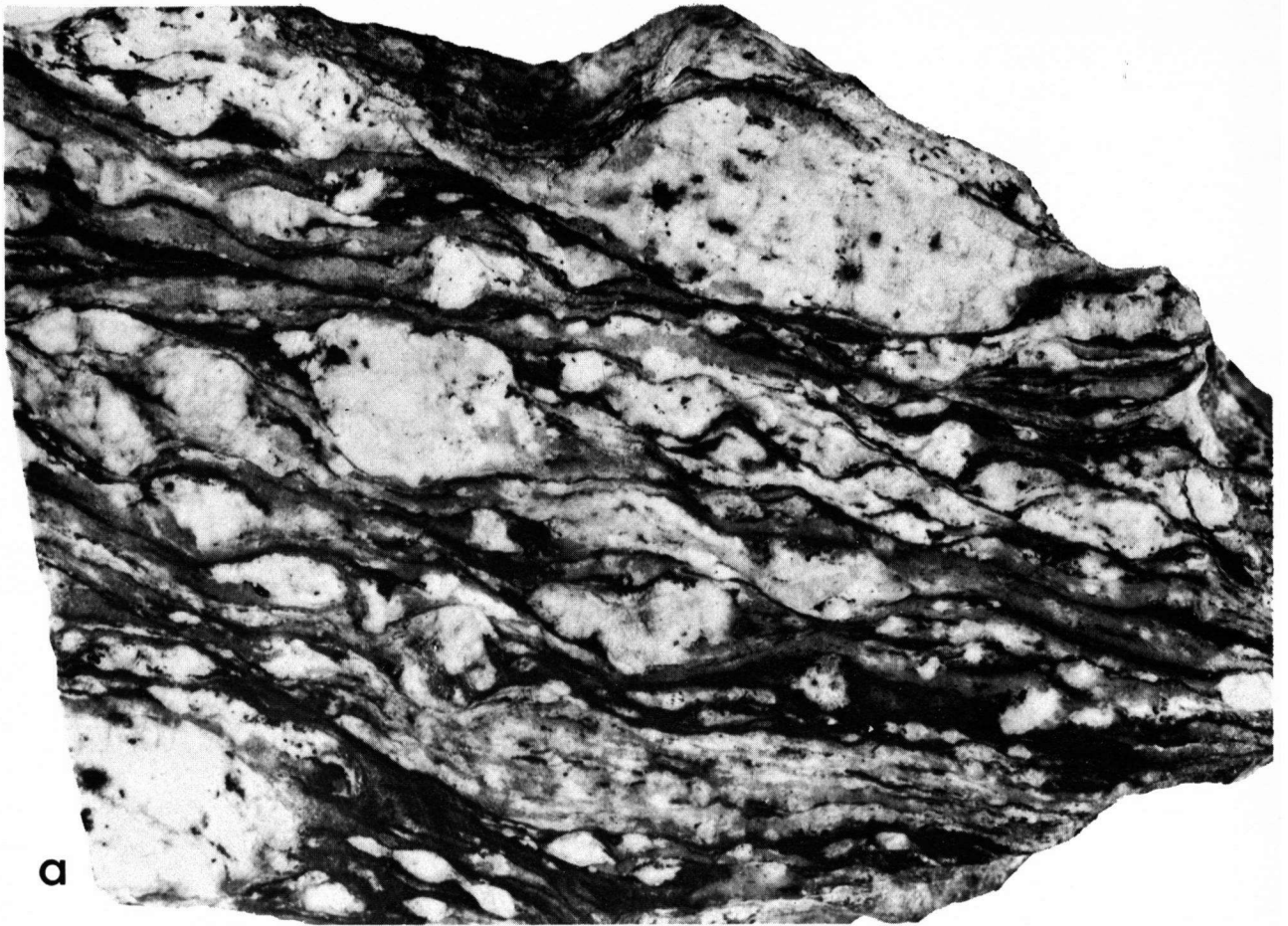


**PLATE VIII**

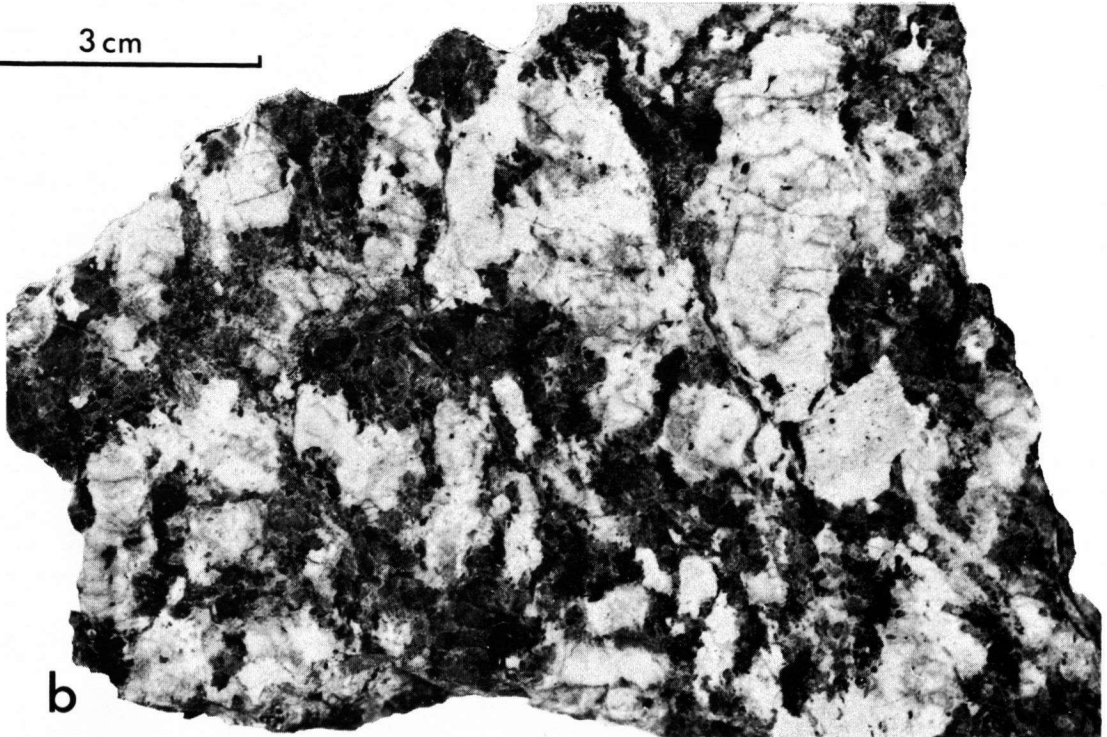
- a. Coarse-grained augengneiss with a phyllonitic and partly mylonitic texture, due to a strong tectonization ( $F_3$ ) after migmatization (St. 141781).**
- b. Coarse-grained augengneiss after migmatic recrystallization into a very coarse-grained two-mica granite, 2.5 km SE of Esteiro.**





**a**

3 cm



**b**

#### PLATE IX

- a. The megacrystal-bearing granodiorite has become a kalyrite as a result of  $F_3$  and fault movements. Most of the quartz has been squeezed out. Mt. Tállara, S of Noya.
- b. Photomicrograph (crossed nicols) of a late-stage muscovite in a medium to fine-grained two-mica granite (Muros-type). Phyllonitization ( $F_3$ ) has affected the granite and the muscovite (St. 141829).
- c. A highly deformed two-mica granite near the fault 1 km WSW of Boiro. Quartz has filled up the fractures in the alkali feldspar and has also recrystallized into polygonal aggregates. Photomicrograph, crossed nicols.

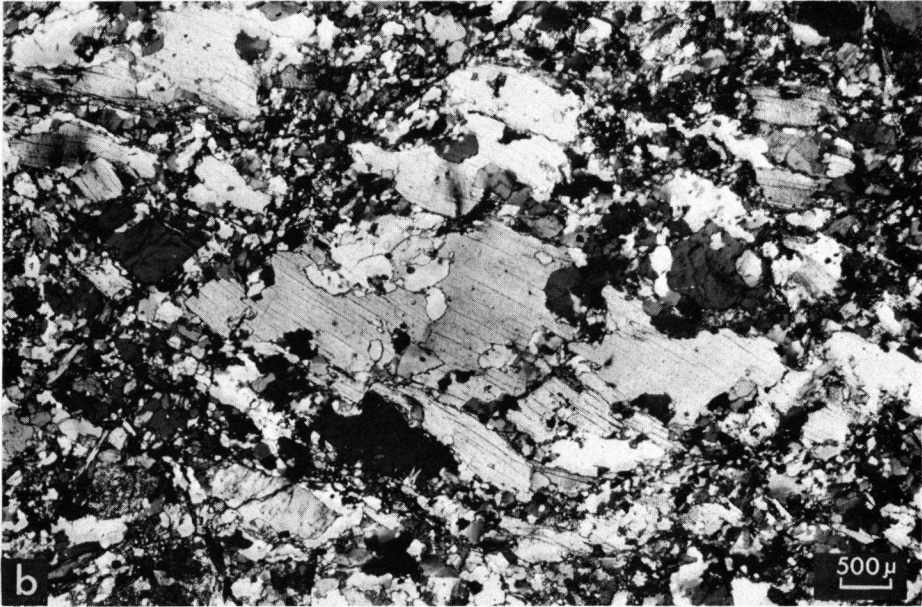
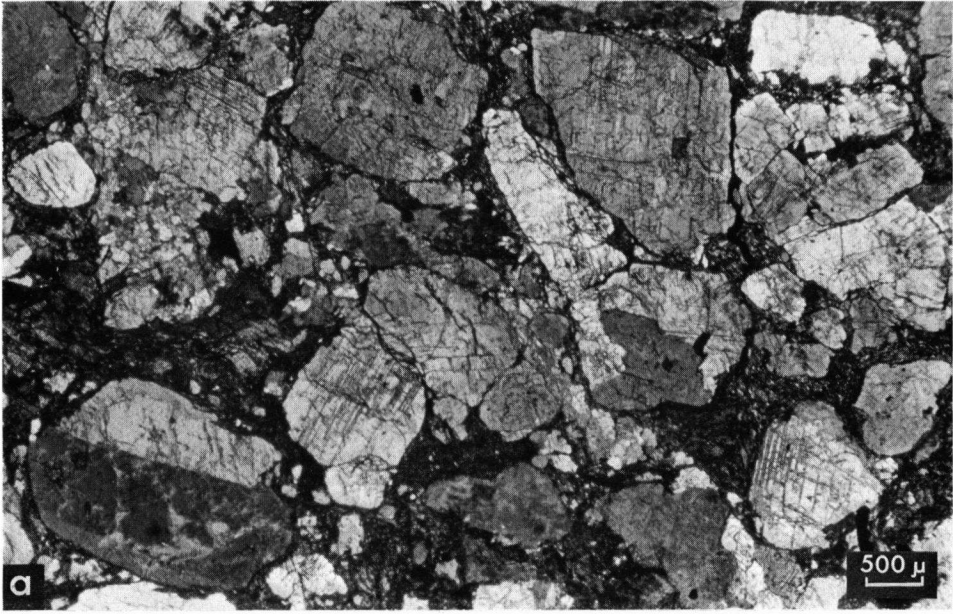


## PLATE X

- a. Paragneiss xenolith in the megacrystal-bearing granodiorite. Relatively large plagioclase crystals are the result of metasomatism (St. 141791).
- b. A cognate hornblende-biotite diorite inclusion in the megacrystal-bearing granodiorite. Note the large (only slightly deformed) biotite flakes in contrast to the more finely grained hornblende and plagioclase (St. 141792).
- c. Highly phyllonitic and partly mylonitic megacrystal-bearing granodiorite (F<sub>3</sub>). Quarry at Pta. Requeixo.
- d. Muscovite granite (phyllonitic), a relatively late-magmatic product of the megacrystal-bearing granodiorite series (St. 141809).

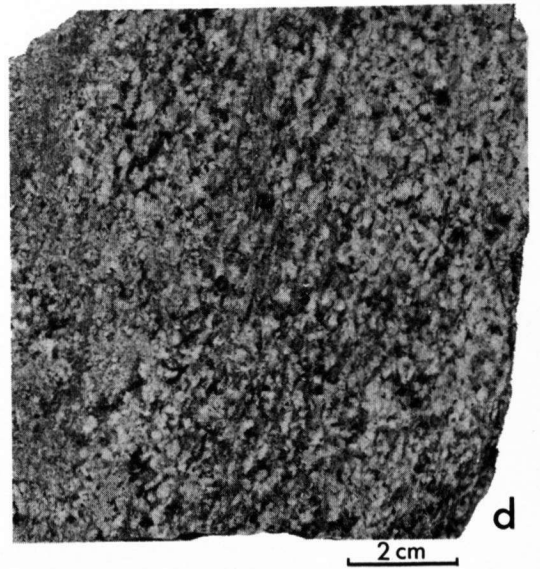
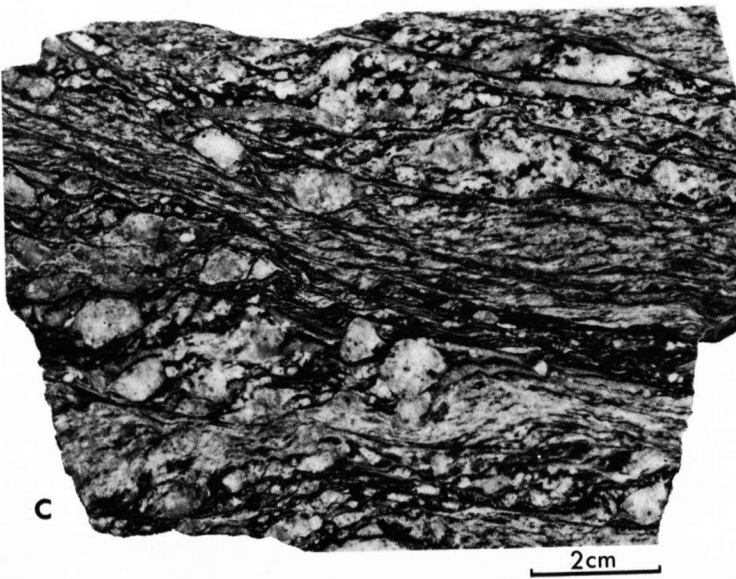
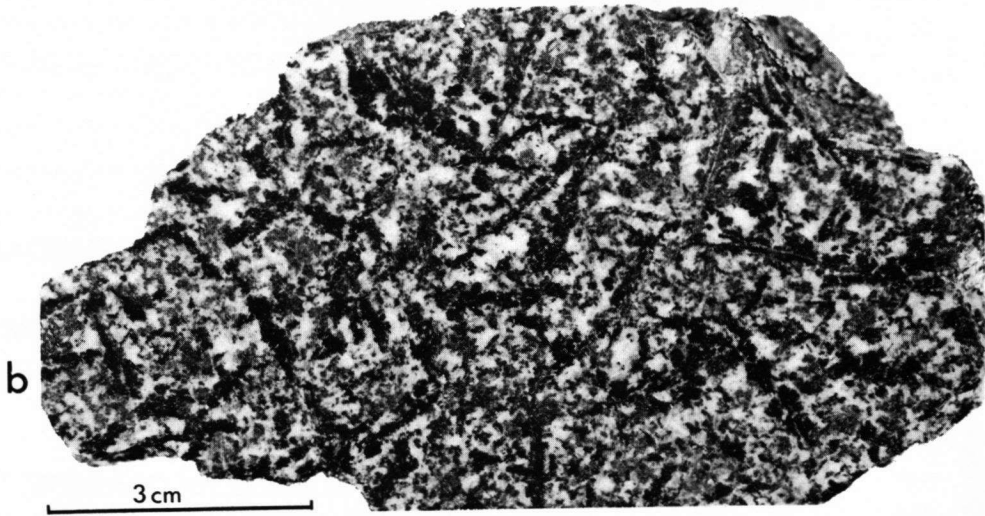
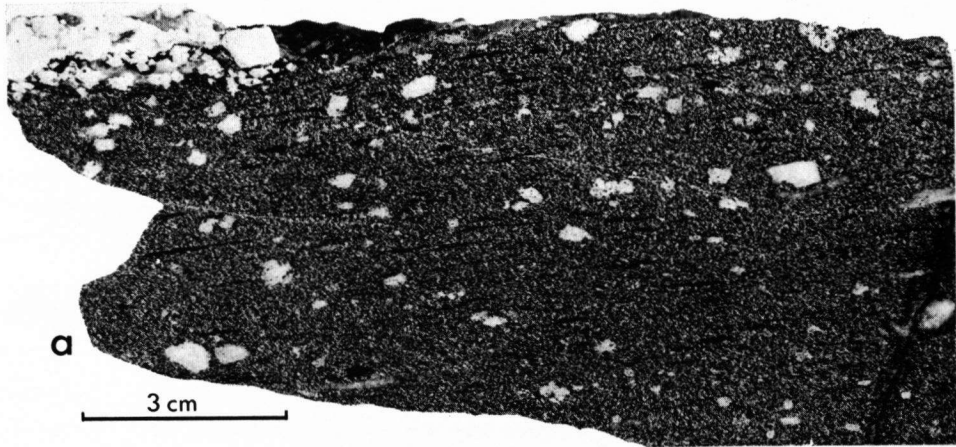
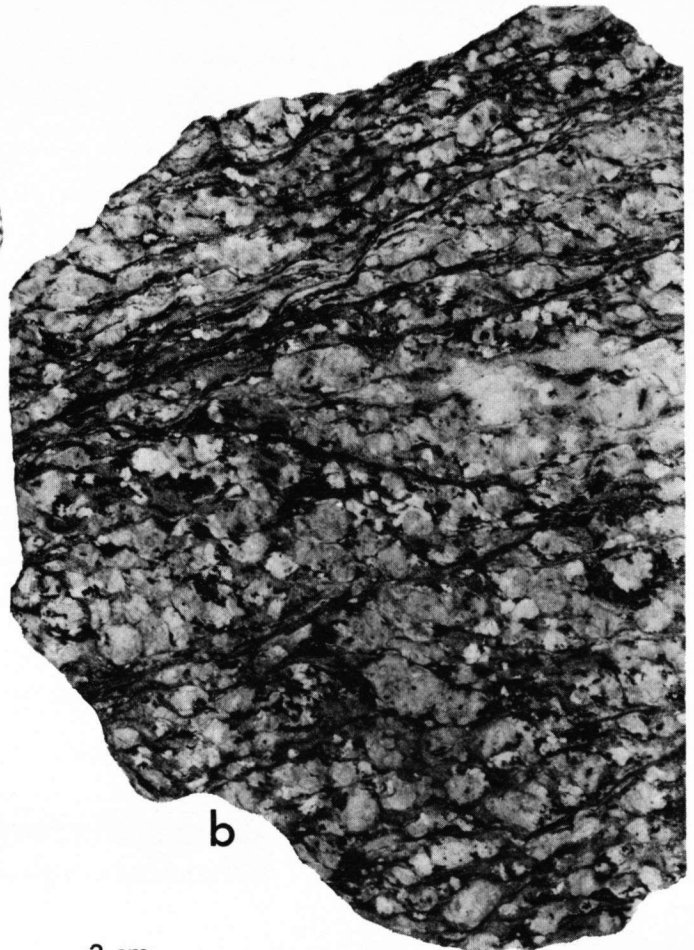
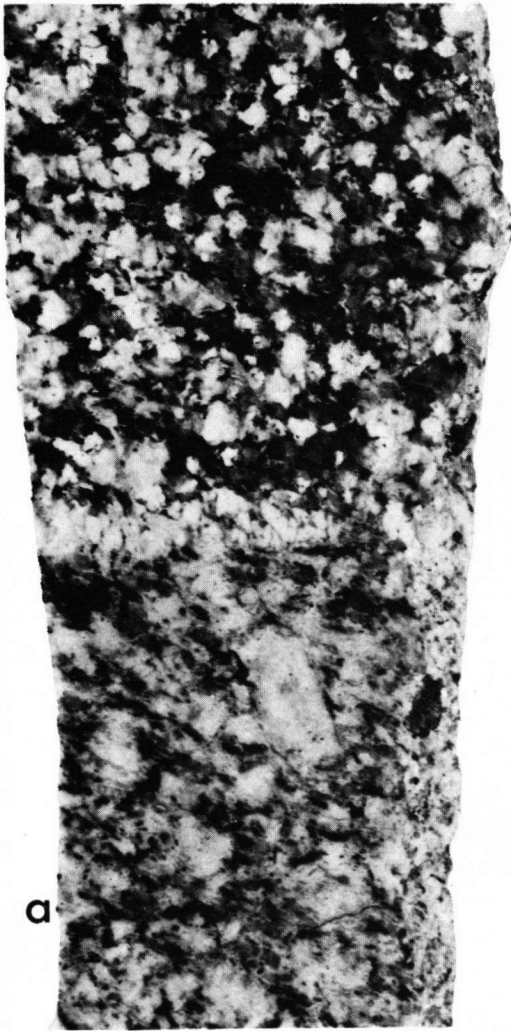


**PLATE XI**

- a. Two varieties of the medium to coarse-grained two-mica granite (Barbanza-type): the older muscovite-rich type (below) and the biotite-rich type (above); samples St. 141822 and St. 141823, respectively.
- b. The medium to coarse-grained Barbanza two-mica granite (St. 141827), often inhomogeneous and locally phyllonitic.
- c. The medium-grained two-mica granite (Banza-type) containing a fine-grained two-mica granite inclusion (St. 141831). Both granites are cut off by a pegmatite.



3 cm

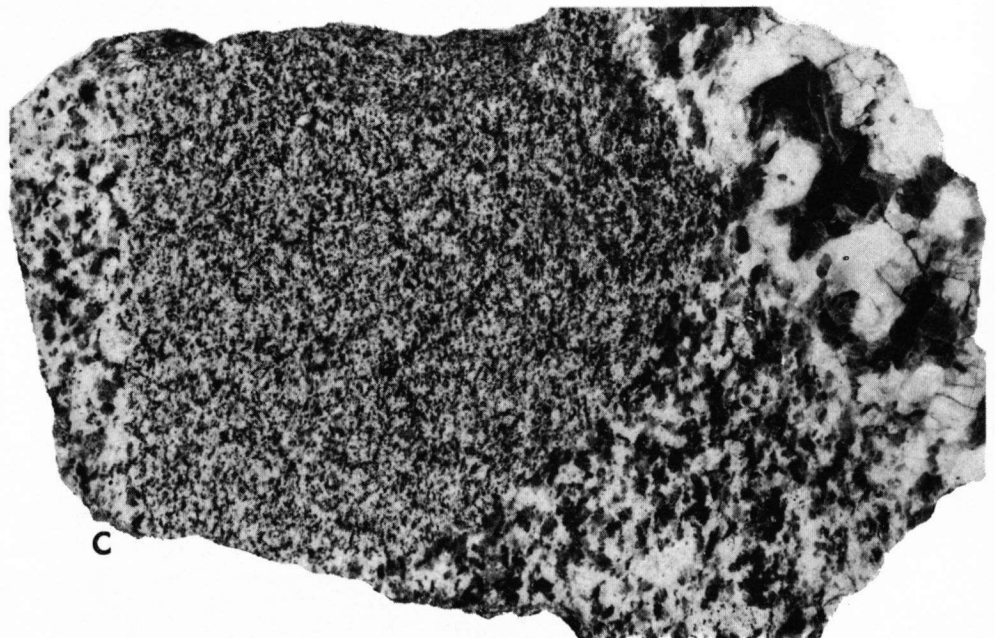
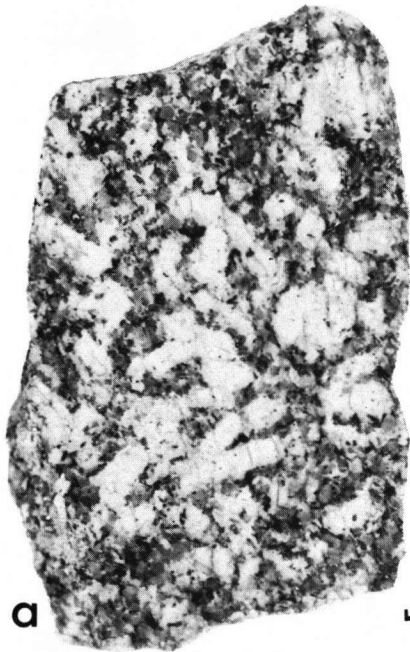


**PLATE XII**

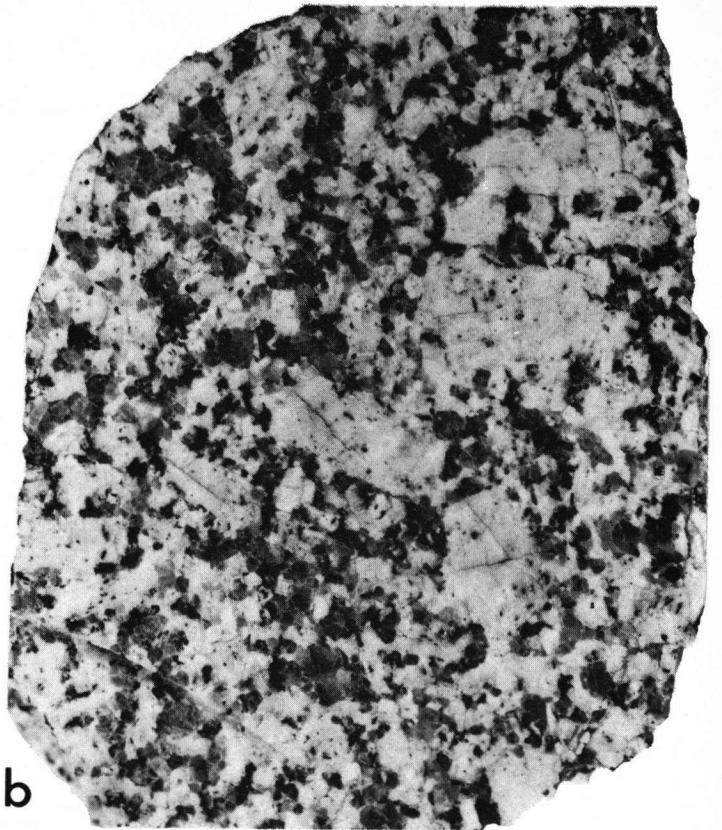
- a. The late syn-kinematic megacrystal-bearing Ruña two-mica granite (St. 141839).
- b. The post-kinematic Arbos granite, a coarse-grained megacrystal-bearing two-mica granite (St. 141855).
- c. The post-kinematic Pando granite, a medium to coarse-grained slightly porphyritic biotite granite (St. 141817).
- d. The post-kinematic Caldas de Reyes granite, a coarse-grained slightly porphyritic amphibole-bearing biotite granite (St. 141814).



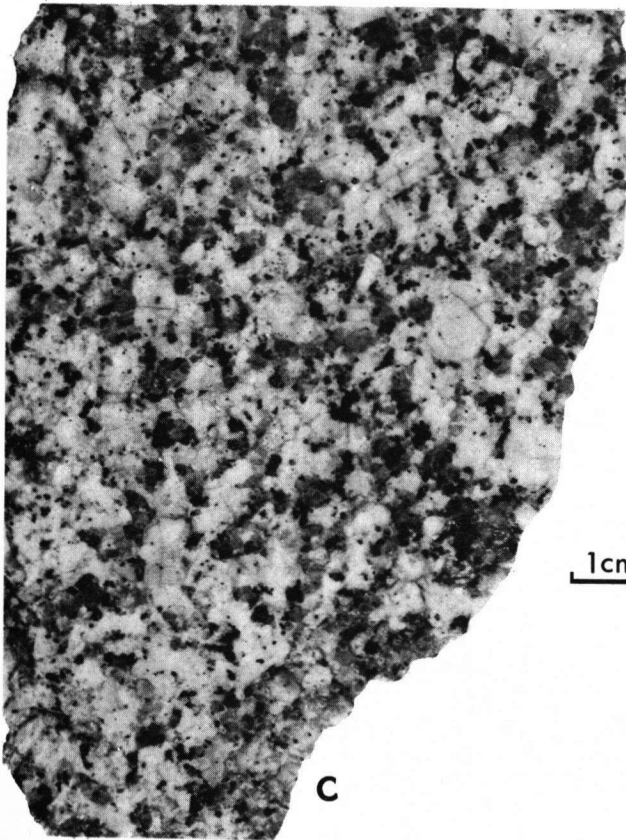


a

1cm

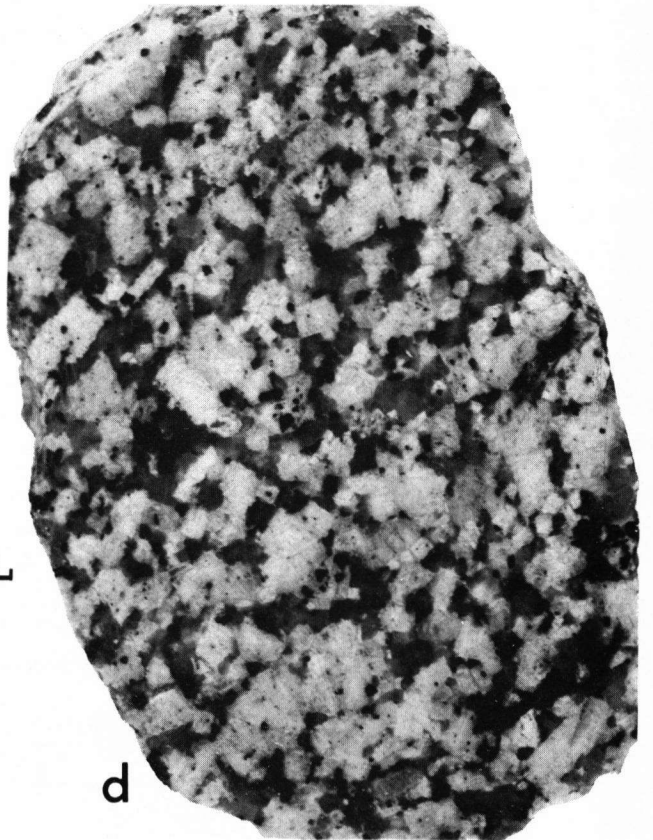


b



c

1cm



d

### PLATE XIII

Zircons from biotite orthogneiss:

- a. Zircon showing an interrupted growth (St. 141717,  $\times 160$ ).
- b. Oblong crystal from same sample with the forms  $\{101\}$  and  $\{110\}$ . Magn.  $160 \times$ .

Zircons from biotite-ferrohastingsite orthogneiss:

- c. Crystal with damaged faces. Note the presence of  $\{301\}$  in addition to  $\{101\}$  and  $\{100\}$ . Magn.  $242 \times$  (Stereoscan, photo 11372, Centr. Lab. TNO, Delft).
- d. Composite zircon from same sample. Magn.  $121 \times$  (Stereoscan, photo 11374, Centr. Lab. TNO, Delft).
- e. Heavily resorbed crystal showing an interrupted growth (St. 141860,  $\times 400$ ).
- f. Resorbed crystal with inclusions concentrated in the rim. (St. 141860,  $\times 160$ ).
- g. Zircon aggregate consisting of three intergrown crystals and a core. Magn.  $160 \times$ .
- h. Zoned zircon with core crowded with inclusions. A small zircon inclusion is oriented  $\parallel \{101\}$ . The contours clearly reveal the presence of  $\{301\}$ , this form is not visible in the core. Magn.  $320 \times$ .
- i. Zircon from amphibole-bearing biotite orthogneiss. (St. 141727,  $\times 320$ ).

Zircons from migmatic biotite orthogneiss:

- j. A crystal showing the forms  $\{101\}$ ,  $\{100\}$  and (subordinate)  $\{110\}$ . The numerous inclusions are seemingly not oriented. The upper part of the crystal is overgrown due to migmatic recrystallization (St. 141789,  $\times 240$ ).
- k. Most of the crystals are heavily resorbed and have smooth surfaces (St. 141789,  $\times 200$ ).

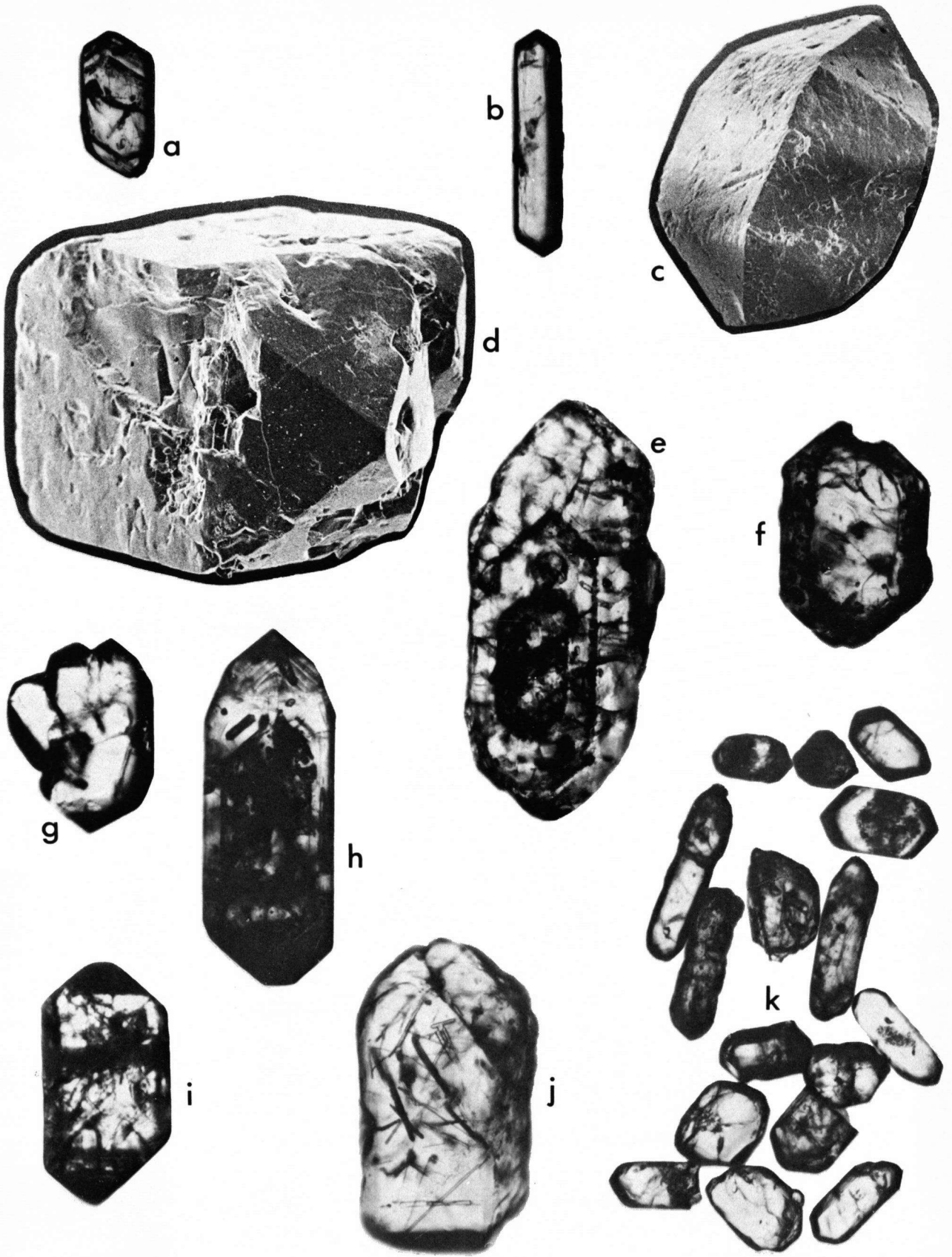


#### PLATE XIV

##### Zircons from coarse-grained augengneisses:

- a. A crystal displaying the forms  $\{101\}$ , somewhat subordinate  $\{211\}$  and  $\{110\}$ . The crystal edges are only slightly resorbed. Magn.  $110 \times$  (Stereoscan, photo 11379, Centr. Lab. TNO, Delft). Sample St. 141781.
- b. A zircon with the important form  $\{211\}$  as well as  $\{101\}$ ,  $\{110\}$  and subordinate  $\{100\}$ ; also a heavily resorbed monazite crystal. Magn.  $220 \times$  (Stereoscan, photo 11376, Centr. Lab. TNO, Delft). Same Sample.
- c. Egg-shaped clear crystal with  $\{211\}$  as an important face (St. 141783,  $\times 160$ ).
- d. Oblong and partially zoned crystal (St. 141781,  $\times 160$ ).
- e. Highly elongated and highly resorbed crystal. (St. 141778,  $\times 160$ ).
- f. Zircon with aberrant shape enclosing a normal core (St. 141778,  $\times 160$ ).
- g. Zircon with a rounded, probably sedimentary, zircon core (St. 141778,  $\times 160$ ).
- h. Zircon aggregate with resorbed core and euhedral overgrowth (St. 141783,  $\times 160$ ).
- i. Resorbed crystal with an aberrant morphology (St. 141782,  $\times 160$ ).
- j. Clear and euhedral crystal (St. 141781,  $\times 160$ ).
- k. Euhedral crystals; the large crystal displays the forms  $\{211\}$ ,  $\{100\}$  and  $\{110\}$ , while  $\{101\}$  is absent. Magn.  $110 \times$  (Stereoscan, photo 11380, Centr. Lab. TNO, Delft). Sample St. 141781.

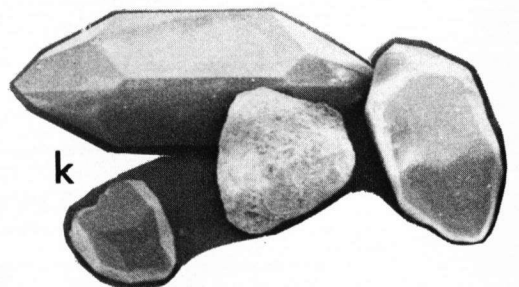
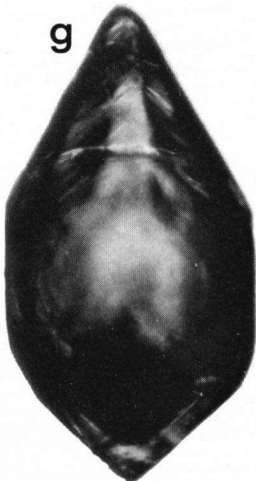
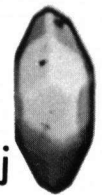
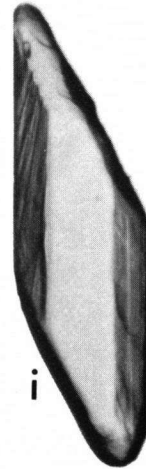
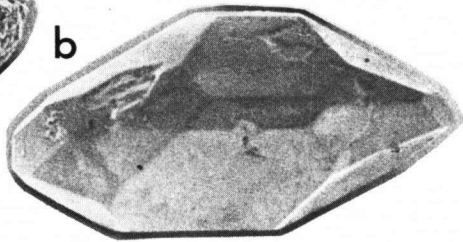
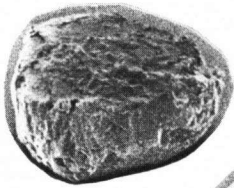
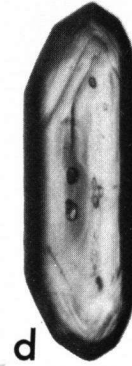
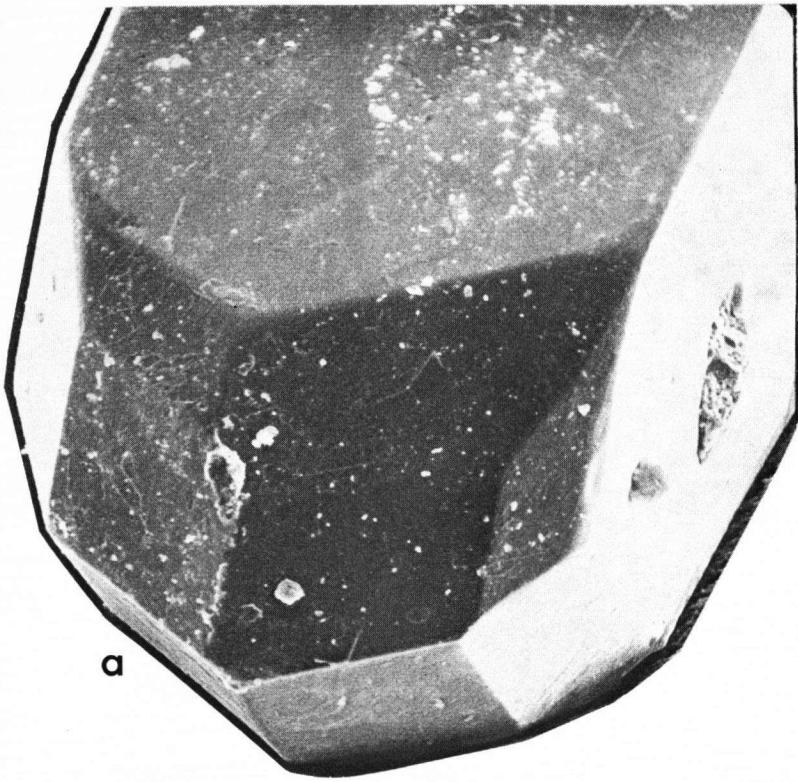
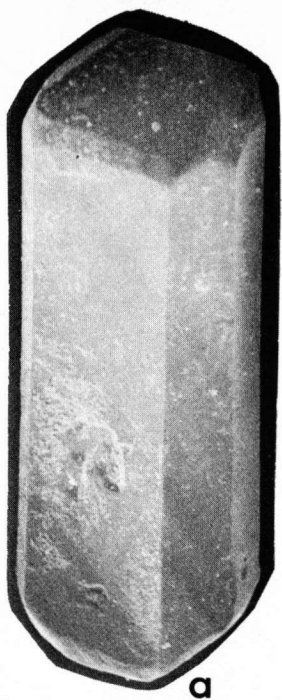


## PLATE XV

Zircons from granodioritic cognate inclusions belonging to the megacrystal-bearing granodiorite series:

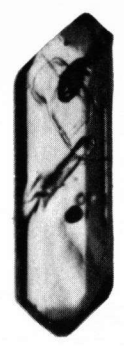
- a. A zircon with an aberrant pseudo-rhombic shape, displaying the crystal forms {101}, {100}, subordinate {301}, subordinate {211} and {110}. Magn. 770 × (Stereoscan, photo 11388, Centr. Lab. TNO, Delft).
  - b. A broken crystal with the forms {101}, {100} and {110}. Magn. 990 × (Stereoscan, photo 11383, Centr. Lab. TNO, Delft).
  - c. Euhedral crystal with different inclusions. Magn. 160 ×.
  - d. Isometric zircon crystal with the shape of a dodecahedron. Magn. 320 ×.
  - e. Oblong crystal with aberrant shape: breadth > thickness. Magn. 160 ×.
  - f. An early-broken-later-healed zircon crystal that survived mechanical crushing. Magn. 569 ×.
- (Photos a-f are from sample St. 141795; photos g-i from sample St. 141793).
- g. A highly resorbed zircon aggregate. Magn. 160 ×.
  - h. Highly resorbed crystal with gaseous and two-phase inclusions. Magn. 300 ×.
  - i. Highly resorbed crystals with two-phase inclusions, showing evidence of a hindered growth. Magn. 160 ×.



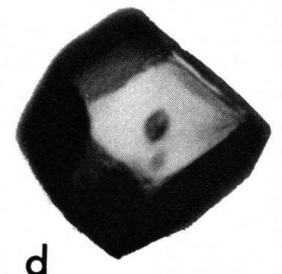
a



b



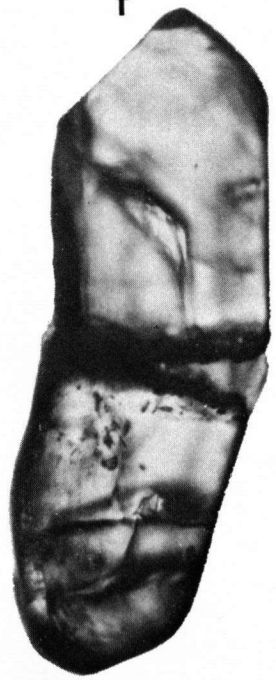
c



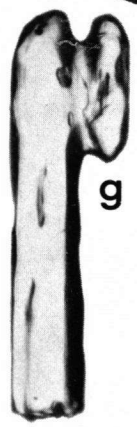
d



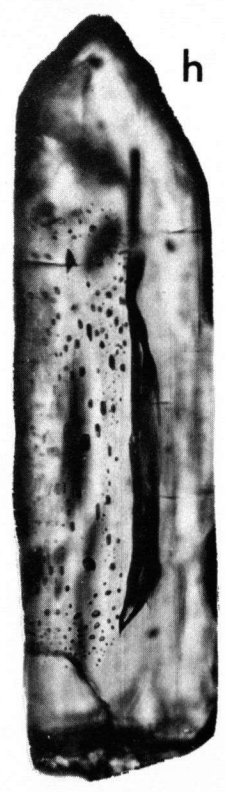
e



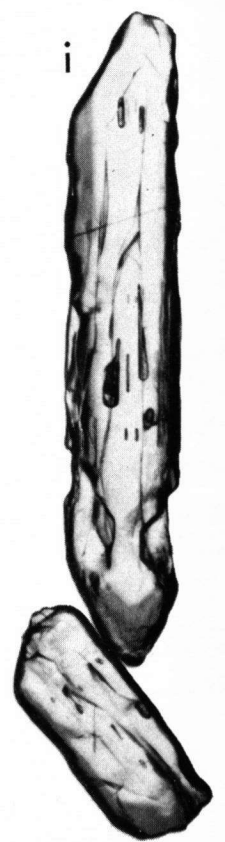
f



g



h



i

## PLATE XVI

Zircons from megacrystal-bearing granodiorite and muscovite granite:

- a. Aberrant shape {211} as an important crystal form (St. 141804, × 160).
- b. Oblong crystal with resorbed core (St. 141861, × 160).
- c. Zoned crystal with inclusions attached to growth zones (St. 141804, × 200).
- d. and e. Aberrant shapes often present in the megacrystal-bearing granodiorite (St. 141861, × 240).
- f. Resorbed zircon aggregate (St. 141804, × 200).
- g. Clear evidence of a hindered growth. Crystal form {101} is subordinate or absent (St. 141861, × 160).
- h. Resorbed zircon with turbid core and finely zoned rim from muscovite granite (St. 141809, × 240).
- i. Heavily resorbed euhedral monazite crystal (St. 141805, × 400).
- j. Heavily resorbed xenotime partly enclosing a zircon (St. 141805, × 400).
- k. Euhedral brookite crystal (St. 141776, × 160).
- l. Euhedral anatase crystal (St. 141776, × 160).
- m. Fibrolitic anatase (St. 141776, × 160).



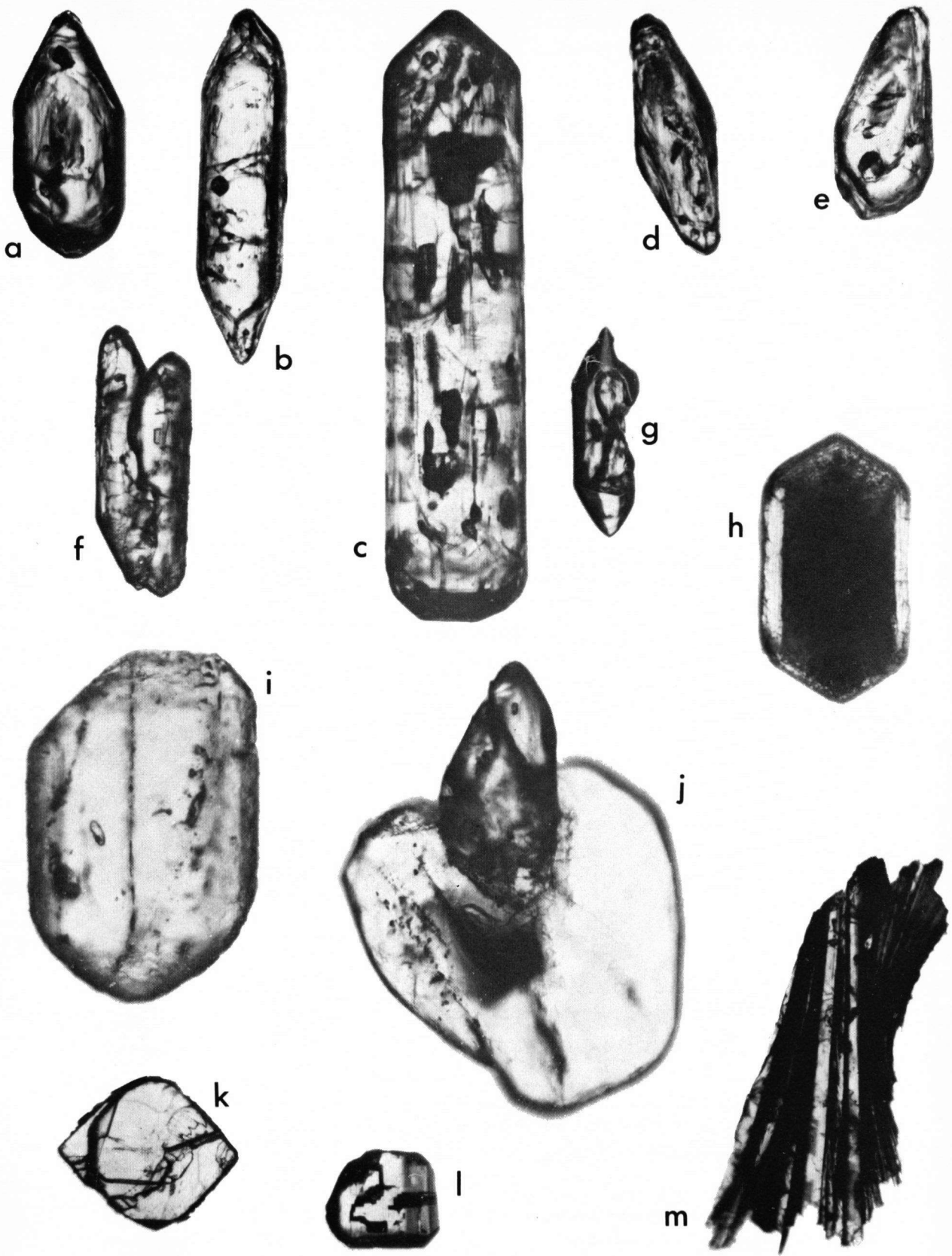


## PLATE XVII

a. "Sedimentary" zircons from metaquartzite (St. 141699,  $\times 220$ ).

Zircons from migmatites:

b. Resorbed "sedimentary" zircons with outgrowths; pegmatoid metatect of a migmatite. Magn.  $160 \times$ .

c. Resorbed zircon grains in restite (St. 141776,  $\times 160$ ).

d, e and f. Resorbed zircons with newly formed outgrowths from paragneiss migmatite (St. 141773,  $\times 160$ ).

g, h and i. Regenerated zircons from metatect of an inhomogeneous diatexite (St. 141776).

Zircon from photo h encloses two sedimentary cores. Magn.  $160 \times$ ,  $240 \times$  and  $500 \times$ , respectively.

Note the differences with respect to the zircons from the restite of the same sample (photo c).

Zircons from granitoid migmatite (see Chapter I, Fig. 1-27):

j. Euhedral crystal with irregular outgrowth. Magn.  $300 \times$ .

k. Zircon aggregate with resorbed cores and overgrowths. Magn.  $160 \times$ .

l. and m. Newly grown euhedral crystals with the forms  $\{101\}$ ,  $\{211\}$ ,  $\{100\}$  and  $\{110\}$ . Magn.  $160 \times$ .

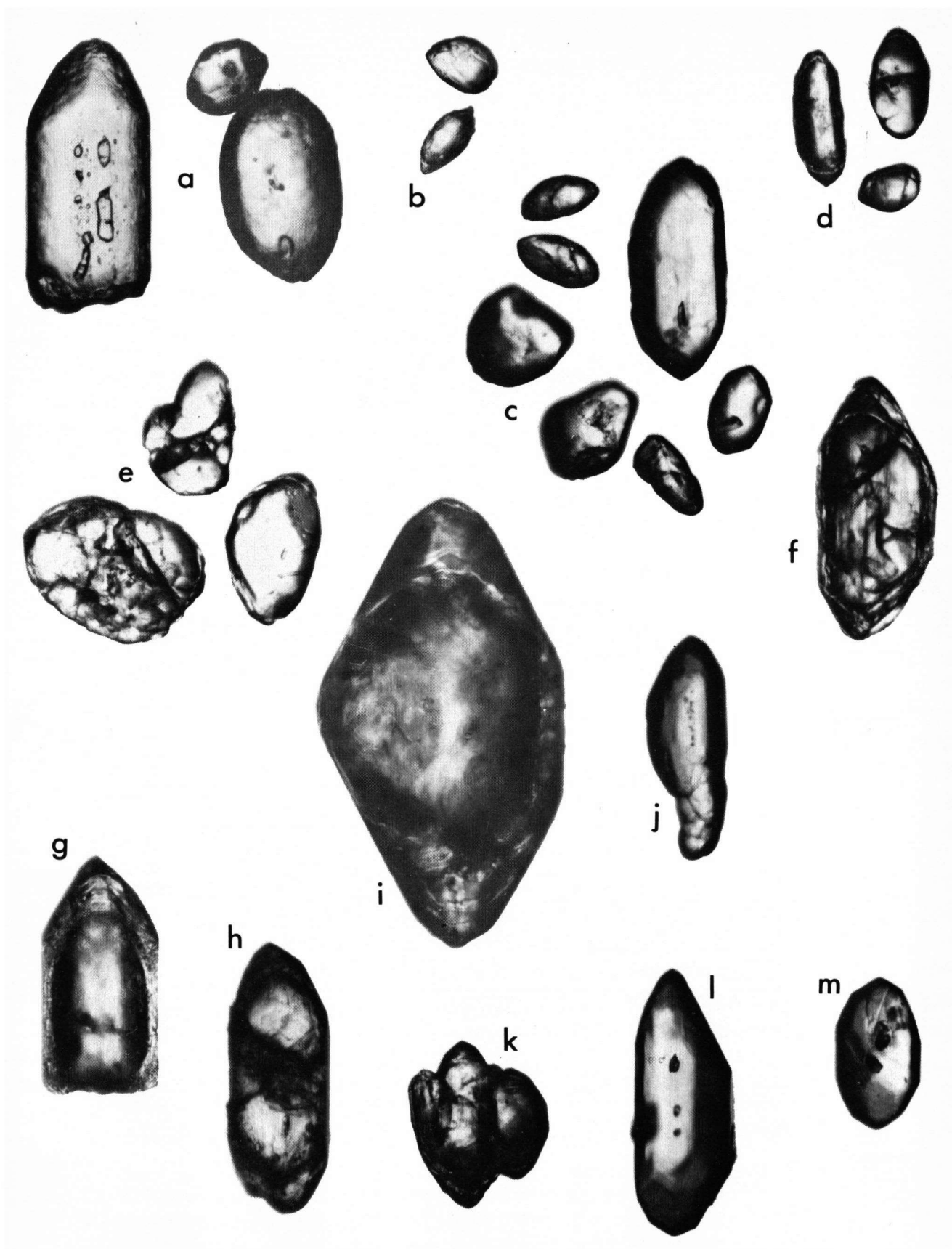


## PLATE XVIII

### Zircons from two-mica granites:

- a. An oval-shaped crystal from the Banza granite. Magn. 160 ×.
- b. Zircon from the Barbanza granite; form {101} is (almost?) absent (St. 141824, × 160).
- c. and d. Oblong crystals from eastern two-mica granites. Zircon d is zoned with inclusions attached to the growth-zones. Magn. 160 × and 240 ×, respectively (St. 141838 and St. 141837).
- e. Zoned zircon with resorbed core from Barbanza granite. Magn. 400 × (St. 141824).
- f. Regenerated zircon with "sedimentary" zircon core and zoned rim with low birefringence (St. 141821, × 400).
- g. Zircon fragment with numerous small and rounded inclusions; eastern two-mica granite. Magn. 160 ×.
- h. Aberrant crystal shape; eastern two-mica granite (St. 141838, × 160).
- i. Markedly zoned zircon from Ruña granite, a typical feature (St. 141839, × 140).

### Zircons from granite porphyry (St. 141858):

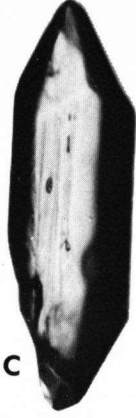
- j. Crystal with the forms {101} and {100}, enclosing smaller zircons and opaque minerals. Magn. 160 ×.
- k, l and m. Aberrant crystal shapes; k: length ≫ breadth ≈ thickness, l and m: length > breadth ≫ thickness. Magn. 160 ×.
- n. Aberrant shape with sharp outlines displaying the forms {101}, {110} and {100}. Magn. 160 ×.
- o. Crystal with the forms {101} and {110}, enclosing a resorbed core. Magn. 300 ×.
- p. Markedly zoned crystal; the prismatic forms in the inner part of the crystal have developed very subordinately. Magn. 400 ×.



a



b

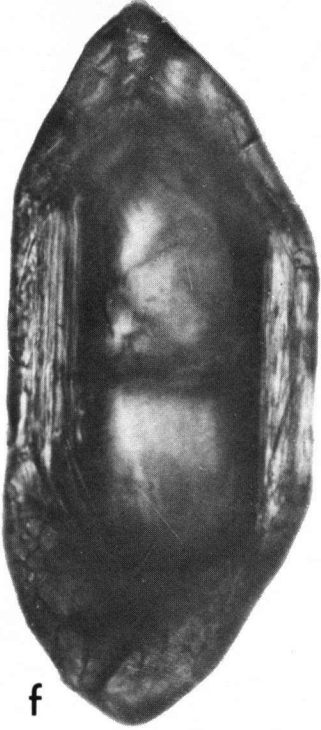
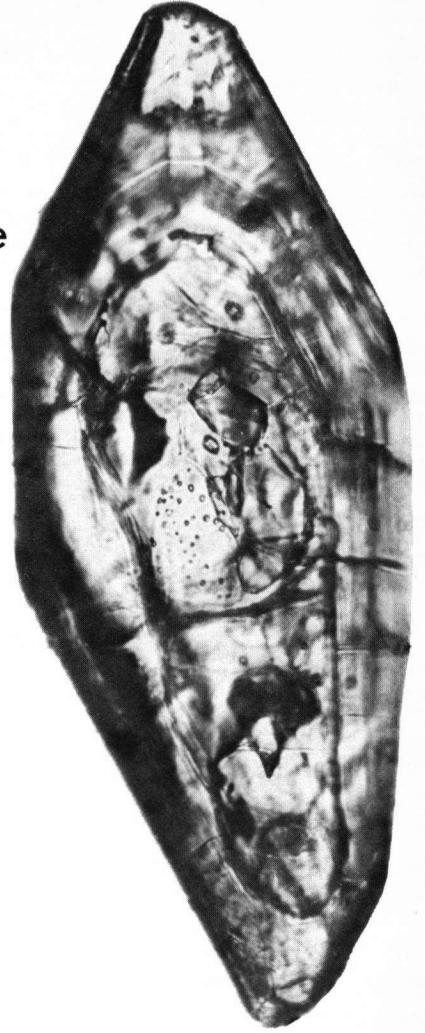


c

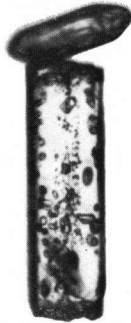


d

e



f



g



h



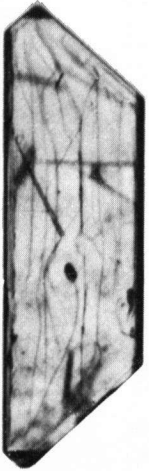
i



j



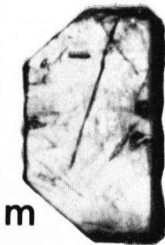
k



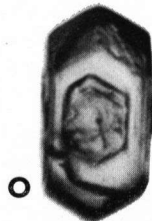
l



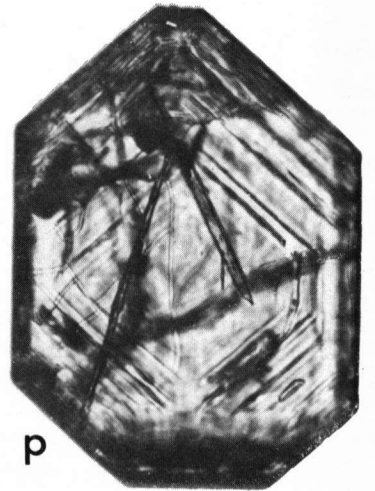
n



m



o



p

## PLATE XIX

Zircons from the post-kinematic Arbos granite:

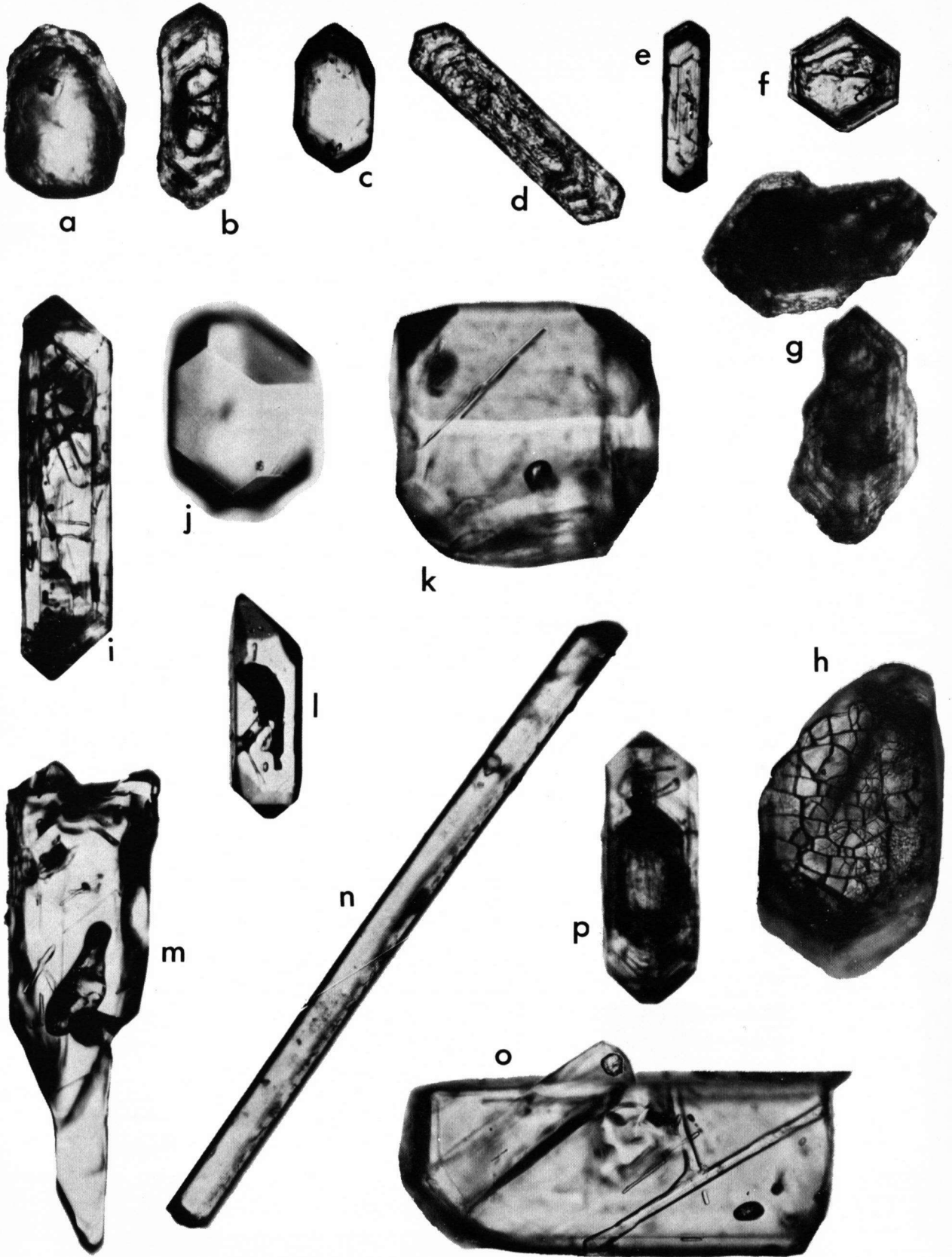
- a. Sedimentary zircon with outgrowth (St. 141854,  $\times 160$ ).
- b. Regenerated zircon with "sedimentary" core and finely zoned rim enclosing a small euhedral zircon (St. 141855,  $\times 160$ ).
- c. Newly grown euhedral crystal (St. 141855,  $\times 160$ ).
- d. Oblong zircon showing a marked zoning and interrupted growth. Magn.  $400 \times$  (St. 141855). A characteristic zircon habit for the Arbos granite.

Zircons from the post-kinematic Pando granite (St. 141816):

- e. Zoned zircon with the forms  $\{101\}$  and  $\{110\}$ . Magn.  $160 \times$ .
- f. Equidimensional zircon displaying an interrupted growth. Magn.  $160 \times$ .
- g. Typical zircons from the Pando granite with turbid euhedral and sometimes resorbed cores and finely zoned rims with low birefringence. The fluorescence colour of these cores is usually green. Magn.  $220 \times$ .
- h. Microcracks on a crystal surface. The fractures are the result of expansion caused by metamictization. Magn.  $340 \times$ .

Zircons from the post-kinematic Caldas de Reyes granite (mainly St. 141863):

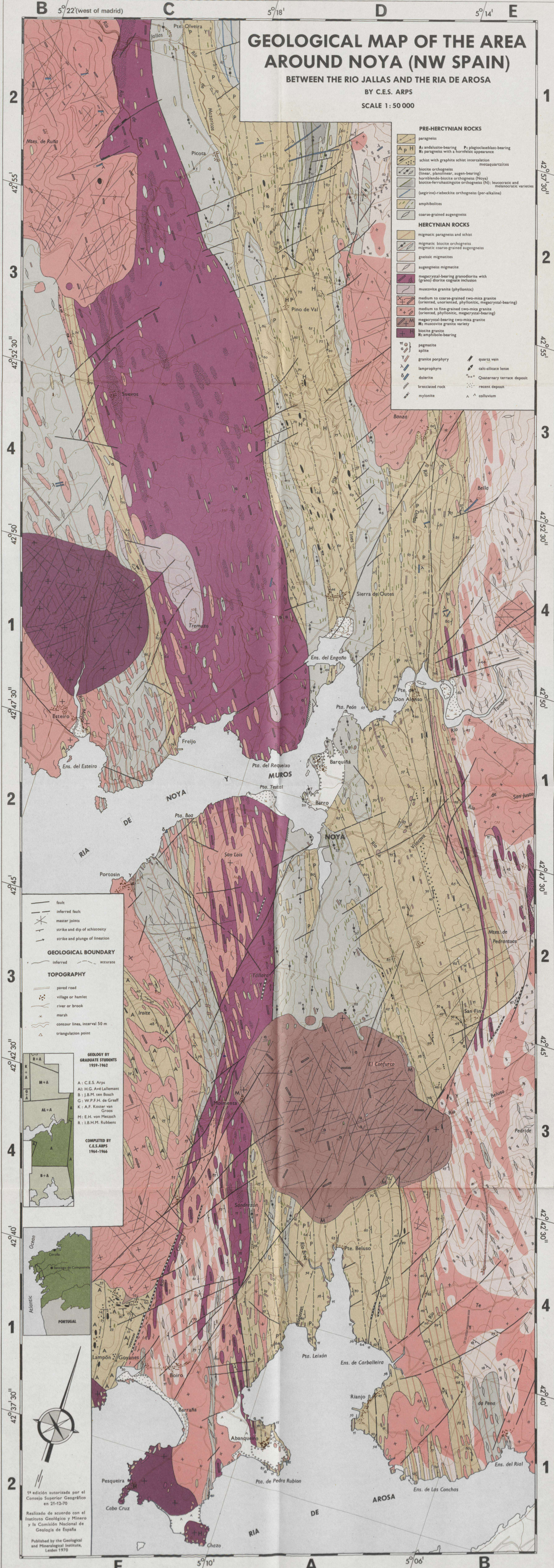
- i. Crystal with core of same shape and many inclusions. Magn.  $160 \times$ .
- j. Euhedral zircon with the forms  $\{101\}$ ,  $\{110\}$  and  $\{100\}$ . Magn.  $160 \times$ .
- k. Aberrant crystal with the forms  $\{101\}$ ,  $\{100\}$  and subordinate  $\{110\}$ . Magn.  $400 \times$ .
- l. Crystal with gaseous and liquid inclusions. Magn.  $160 \times$ .
- m. Irregular crystal shape due to a hindered growth enclosing gaseous and liquid inclusions. Magn.  $160 \times$ .
- n. Aberrant shape: length  $\gg$  breadth  $\approx$  thickness. Magn.  $200 \times$  (St. 141813).
- o. Irregular grain with large apatite inclusion and liquid canals. Magn.  $300 \times$ .
- p. Zoned zircon with turbid core. Magn.  $300 \times$ .



# GEOLOGICAL MAP OF THE AREA AROUND NOYA (NW SPAIN)

BETWEEN THE RIO JALLAS AND THE RIA DE AROSA

BY C.E.S. ARPS  
SCALE 1:50 000



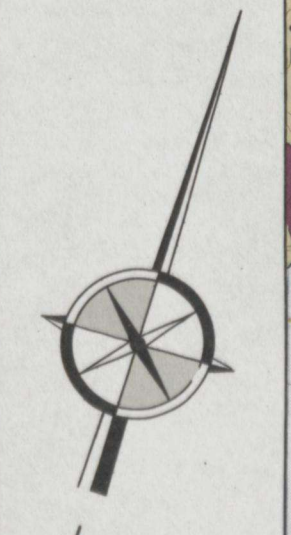
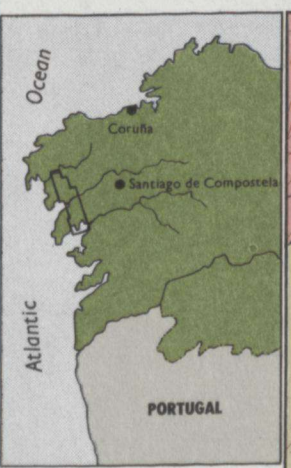
- PRE-HERCYNIAN ROCKS**
- paragneiss
  - A: andalusite-bearing P: plagioclase-bearing
  - H: paragneiss with a hornfelsic appearance
  - schist with graphite schist intercalation
  - metaquartzites
  - biotite orthogneiss (linear, planoliner, augen-bearing)
  - hornblende-biotite orthogneiss (Noya)
  - biotite-ferrohaastingsite orthogneiss (N): leucocratic and microcratic varieties
  - (aegirine)-riebeckite orthogneiss (per-alkaline)
  - amphibolites
  - coarse-grained augengneiss
- HERCYNIAN ROCKS**
- migmatitic paragneiss and schist
  - migmatitic biotite orthogneiss
  - migmatitic coarse-grained augengneiss
  - gneissic migmatites
  - augengneiss migmatite
  - megacrystal-bearing granodiorite with (grano) diorite cognate inclusion
  - muscovite granite (phyllonitic)
  - medium to coarse-grained two-mica granite (oriented, unoriented, phyllonitic, megacrystal-bearing)
  - medium to fine-grained two-mica granite (oriented, phyllonitic, megacrystal-bearing)
  - megacrystal-bearing two-mica granite
  - M: muscovite granite variety
  - biotite granite
  - H: amphibole-bearing
- pegmatite  
 aplite  
 granite porphyry  
 lamprophyre  
 dolerite  
 brecciated rock  
 mylonite
- quartz vein  
 calc-silicate lense  
 Quaternary terrace deposit  
 recent deposit  
 colluvium

- fault
  - inferred fault
  - master joints
  - strike and dip of schistosity
  - strike and plunge of lineation
- GEOLOGICAL BOUNDARY**
- inferred
  - accurate
- TOPOGRAPHY**
- paved road
  - village or hamlet
  - river or brook
  - marsh
  - contour lines, interval 50 m
  - triangulation point

**GEOLOGY BY GRADUATE STUDENTS 1959-1962**

A: C.E.S. Arps  
 Al: H.G. Avé Lallemand  
 B: J.B.M. ten Bosch  
 G: W.P.F.H. de Graaff  
 K: A.F. Koster van Groos  
 M: E.H. von Metzsch  
 R: I.B.H.M. Rubbens

**COMPLETED BY C.E.S. ARPS 1964-1966**



1ª edición autorizada por el Consejo Superior Geográfico en 21-12-70

Realizado de acuerdo con el Instituto Geológico y Minero y la Comisión Nacional de Geología de España

Published by the Geological and Mineralogical Institute, Leiden 1970



		S, SW and W unit	western migmatic complex	central zone	eastern migmatic complex		
block faulting regional uplift			terrace deposits: Goyanes; Barquiña-Barro; Abanqueiro			Quaternary	
			olivine dolerite		(olivine dolerite)	Tertiary Cretaceous Permian	rejuvenation of relief erosion to peneplain
block faulting		granite porphyries	lamprophyres, granite porphyries	lamprophyres, granite porphyries	lamprophyres, granite porphyries	Carboniferous	
regional updoming	tension	[apophyses] Pando granite: biotite granite	Caldas de Reyes granite: amphibole-bearing biotite granite	[apophyses]		280 ± 11 x 10 <sup>6</sup> years ago (whole rock)	contact metamorphism
wrench-faults mylonitization phyllonitization	(E)NE-(W)SW compression	locally destructive	Arbos granite: megacrystal-bearing two-mica granite	aprites, quartz veins			emplacement of post-kinematic granites Sn-W mineralizations: San Finx, Lampón, etc.
subsidence S, SW and W unit	tension (E)NE-(W)SW compression	weak, non-penetrative	pegmatites, aprites, quartz veins	pegmatites, aprites, quartz veins	pegmatites, aprites, quartz veins	F <sub>3</sub>	retrogradation
			[apophyses] Ruña granite: megacrystal-bearing two-mica granite				intrusion of late syn-kinematic allochthonous two-mica granite
			pegmatites, aprites, quartz veins	pegmatites, aprites, quartz veins	pegmatites, aprites, quartz veins	F <sub>2</sub>	crystallization of micas and andalusite in newly-formed cleavage planes
			Muros granites { fine-grained two-mica granite very fine-grained two-mica granite medium-grained two-mica granite ? } southern two-mica granites	Banza granite { medium-grained two-mica granite fine-grained two-mica granite }		298 ± 10 x 10 <sup>6</sup> years ago (whole rock)	emplacement of syn-kinematic parautochthonous to allochthonous two-mica granites
			Barbanza granites { medium to coarse-grained two-mica granite medium to coarse-grained biotite-bearing muscovite granite }		eastern medium to fine-grained two-mica granites (several generations)		schist xenoliths in Barbanza granite: hornblende-hornfels to alk. feldspar-cordierite hornfels facies of thermo-metamorphism
synthetic faults	tension		pegmatites ↑ fine-grained two-mica granites ↑ aplogranites and pegmatites	[pegmatites] aprites muscovite granite coarse-grained two-mica granite megacrystal-bearing granodiorite dioritic and granodioritic cognate inclusions	pegmatites		albitization of oligoclase metablasts in paragneiss around amphibole-bearing orthogneiss (central zone)
subsidence of central zone along fundamental fault					megacrystal-bearing granodiorites (grano)diorites		emplacement of early syn-kinematic megacrystal-bearing granodiorite series along fundamental faults
			greenschist facies: quartz-andalusite-plagioclase-chlorite facies (epi-mesozonal)	migmatization of metasediments, coarse-grained augengneiss and biotite orthogneiss	migmatization of metasediments, coarse-grained augengneiss, biotite orthogneiss		oligoclase metablastesis in paragneiss; metablastic recrystallization of mylonitic orthogneiss
							Abukuma-type plutonometamorphism
(F <sub>1</sub> is main deformation) mylonitization phyllonitization	(E)NE-(W)SW compression	strong; penetrative	F <sub>1</sub>	coarse-grained augengneiss phyllonitization	linear to planolite granite mylonites mylonitization	F <sub>1</sub>	
			? F <sub>0</sub>		gneissic granites ?	F <sub>0</sub> ?	
			[basic in/extrusions]		biotite-ferrohastingsite granite, per-alkaline granite basic dyke swarms [apophyses] (hornblende-) biotite granites	Upper Ordovician: 430-460 x 10 <sup>6</sup> years ago (whole rock)	emplacement of granites along fundamental faults
			sedimentation of pelitic and quartzitic rocks	coarse-grained megacrystal-bearing two-mica granite			
				metamorphism (garnet; staurolite; hornblende; micas)		Early Paleozoic	
				geosynclinal sedimentation of greywackes, pelitic and quartzitic rocks with calcareous intercalations		Precambrian	Barrow-type metamorphism ?
			S, SW and W unit	western migmatic complex	central zone	eastern migmatic complex	

epi-mesozonal → epizonal  
mesozonal → epizonal  
epi-mesozonal → epizonal  
mesozonal → epizonal

HERCYNIAN

PRE-HERCYNIAN

Synoptic chronological table for geological events in the area around Noya (NW Spain)

[apophyses]: present, but (very) subordinate

sample numbers	constituent minerals	quartz	anorthite %	plagioclase	alkali feldspar	biotite	muscovite	andalusite	sillimanite	fabric
700	opaque/ore mineral zircon	+								
701	monazite/xenotime apatite fluorite titanite rutile anatase/brookite tourmaline garnet graphite andalusite sillimanite staurolite biotite chlorite muscovite sericite quartz alkali feldspar/adarlia plagioclase	+								
702										
703										
704										
705										
706										
707										
708										
709										
710										
711										
712										
713										
714										
715										
716										
717										
718										
719										
720										
721										
722										
723										
724										
725										
726										
727										
728										
729										
730										
731										
732										
733										
734										
735										
736										
737										
738										
739										
740										
741										
742										
743										
744										
745										
746										
747										
748										
749										
750										
751										
752										
753										
754										
755										
756										
757										
758										
759										
760										
761										
762										
763										

Table I-1 - Non-migmatic gneisses and schists

sample numbers	constituent minerals	quartz	anorthite %	plagioclase	alkali feldspar	biotite	muscovite	andalusite	sillimanite	fabric
711	opaque/ore mineral zircon apatite fluorite titanite pyrochlore xenotime tourmaline garnet astrophyllite sericite riebeckite ferrosodite hornblende ferrosalite blue-green hornblende epidote/clinozoisite allanite biotite chlorite muscovite/sericite quartz alkali feldspar plagioclase	+								
712										
713										
714										
715										
716										
717										
718										
719										
720										
721										
722										
723										
724										
725										
726										
727										
728										
729										
730										
731										
732										
733										
734										
735										
736										
737										
738										
739										
740										
741										
742										
743										
744										
745										
746										
747										
748										
749										
750										
751										
752										
753										
754										
755										
756										
757										
758										
759										
760										
761										
762										
763										

Table I-2 - Biotite orthogneisses and amphibole-bearing orthogneisses

sample numbers	constituent minerals	quartz	anorthite %	plagioclase	alkali feldspar	biotite	muscovite	andalusite	sillimanite	fabric
704	opaque/ore minerals zircon monazite/xenotime apatite fluorite titanite rutile anatase/brookite tourmaline garnet sillimanite beryl biotite chlorite muscovite sericite quartz alkali feldspar plagioclase saussurite	+								
705										
706										
707										
708										
709										
710										
711										
712										
713										
714										
715										
716										
717										
718										
719										
720										
721										
722										
723										
724										
725										
726										
727										
728										
729										
730										
731										
732										
733										
734										
735										
736										
737										
738										
739										
740										
741										
742										
743										
744										
745										
746										
747										
748										
749										
750										
751										
752										
753										
754										
755										
756										
757										
758										
759										
760										
761										
762										
763										

Table I-4 - Migmatite metasediments, migmatite coarse-grained gneisses and migmatite biotite orthogneisses

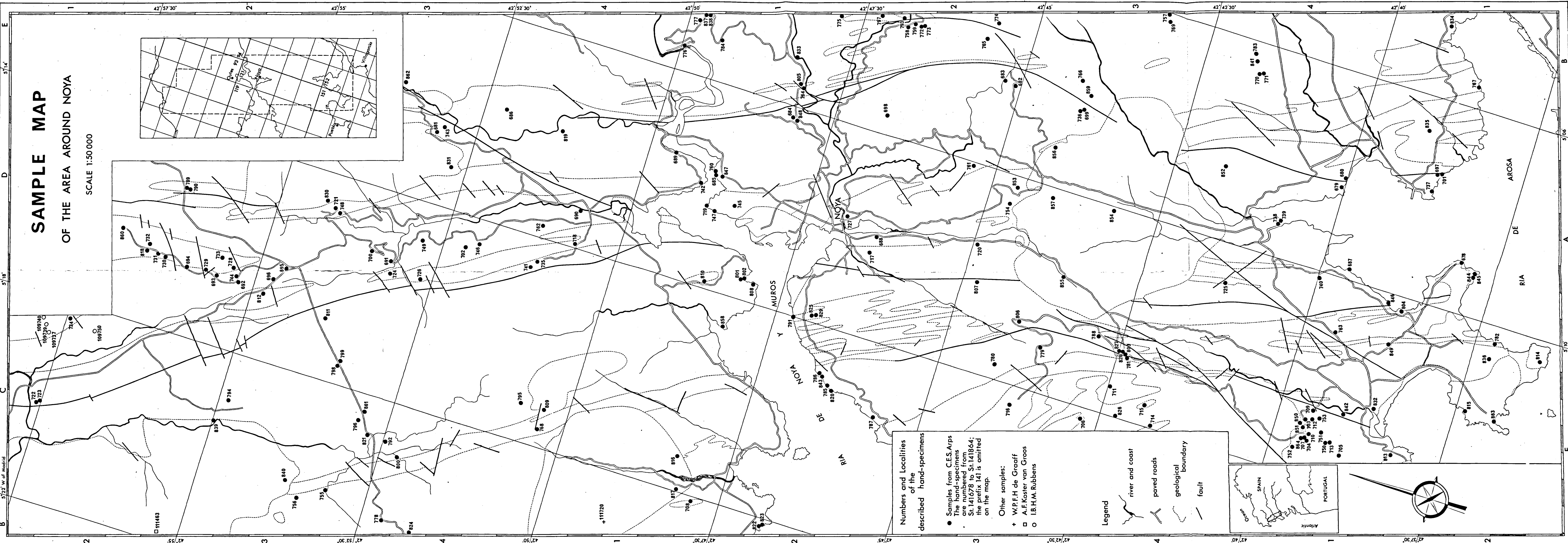
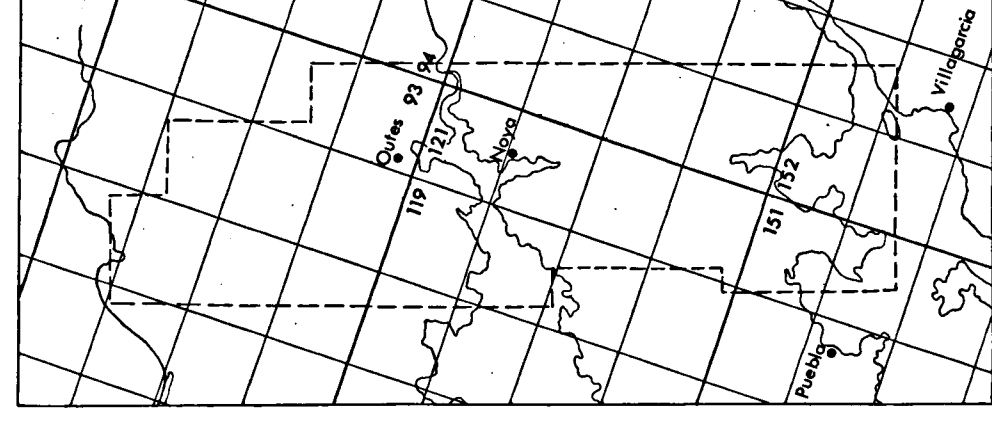
sample numbers	constituent minerals	quartz	anorthite %	plagioclase	alkali feldspar	biotite	zircon	apatite	fabric	
892	opaque/ore minerals zircon monazite/xenotime apatite fluorite titanite rutile anatase/brookite tourmaline beryl garnet olivine pyroxene bl. gr. hornblende, brown hornblende in lamprophyres dark green amphibole clinozoisite/epidote allanite sillimanite biotite chlorite muscovite sericite quartz alkali feldspar plagioclase saussurite calcite	+								
893										
894										
895										
896										
897										
898										
899										
900										
901										
902										
903										
904										
905										
906										
907										
908										
909										
910										
911										
912										
913										
914										
915										
916										
917										
918										
919										
920										

Table I-5 - Megacryst-bearing granodioritic, migmatitic, quartz-apatite, post-kinematic biotite gneisses, amphibolites and a olivine gneiss

sample numbers	constituent minerals	quartz	anorthite %	plagioclase	hornblende	cummingtonite	garnet	fabric
715	opaque/ore minerals zircon apatite titan							

# SAMPLE MAP OF THE AREA AROUND NOYA

SCALE 1:50 000



Numbers and Localities of the described hand-specimens

● Samples from C.E.S.Arps  
The hand-specimens are numbered from Sk.141678 to Sk.141864; the prefix 141 is omitted on the map.

Other samples:

- + W.P.F.H de Graaff
- A.F.Koster van Groos
- I.B.H.M. Rubbens

Legend

- river and coast
- paved roads
- geological boundary
- fault

